(12) INTERNATIONAL APPLICATION PUBLISHED UNDER THE PATENT COOPERATION TREATY (PCT)

(19) World Intellectual Property Organization
International Bureau

(43) International Publication Date
13 February 2025 (13.02.2025)

WIPO | PCT

(10) International Publication Number
WO 2025/035125 A1

(51) International Patent Classification:
A61K 38/20 (2006.01) *C07K 14/54* (2006.01)
A61P 3/10 (2006.01) *A61P 37/00* (2006.01)

(21) International Application Number:
PCT/US2024/041786

(22) International Filing Date:
09 August 2024 (09.08.2024)

(25) Filing Language: English

(26) Publication Language: English

(30) Priority Data:
63/531,847 10 August 2023 (10.08.2023) US

(71) Applicant: **THE CURATORS OF THE UNIVERSITY OF MISSOURI** [US/US]; University of Missouri, 316 University Hall, Columbia, Missouri 65211 (US).

(72) Inventor: **ZAGHOUANI, Habib**; 1608 Brookfield Manor, Columbia, Missouri 65203 (US).

(74) Agent: **BOETTLER, Jeannie** et al.; 120 S. Central Ave., Suite 1600, Clayton, Missouri 63105 (US).

(81) Designated States *(unless otherwise indicated, for every kind of national protection available)*: AE, AG, AL, AM, AO, AT, AU, AZ, BA, BB, BG, BH, BN, BR, BW, BY, BZ, CA, CH, CL, CN, CO, CR, CU, CV, CZ, DE, DJ, DK, DM, DO, DZ, EC, EE, EG, ES, FI, GB, GD, GE, GH, GM, GT, HN, HR, HU, ID, IL, IN, IQ, IR, IS, IT, JM, JO, JP, KE, KG, KH, KN, KP, KR, KW, KZ, LA, LC, LK, LR, LS, LU, LY, MA, MD, MG, MK, MN, MU, MW, MX, MY, MZ, NA, NG, NI, NO, NZ, OM, PA, PE, PG, PH, PL, PT, QA, RO, RS, RU, RW, SA, SC, SD, SE, SG, SK, SL, ST, SV, SY, TH, TJ, TM, TN, TR, TT, TZ, UA, UG, US, UZ, VC, VN, WS, ZA, ZM, ZW.

(84) Designated States *(unless otherwise indicated, for every kind of regional protection available)*: ARIPO (BW, CV, GH, GM, KE, LR, LS, MW, MZ, NA, RW, SC, SD, SL, ST, SZ, TZ, UG, ZM, ZW), Eurasian (AM, AZ, BY, KG, KZ, RU, TJ, TM), European (AL, AT, BE, BG, CH, CY, CZ, DE, DK, EE, ES, FI, FR, GB, GR, HR, HU, IE, IS, IT, LT, LU, LV, MC, ME, MK, MT, NL, NO, PL, PT, RO, RS, SE, SI, SK, SM, TR), OAPI (BF, BJ, CF, CG, CI, CM, GA, GN, GQ, GW, KM, ML, MR, NE, SN, TD, TG).

Published:
— *with international search report (Art. 21(3))*
— *with sequence listing part of description (Rule 5.2(a))*

(54) Title: SUPPRESSION OF TYPE 1 DIABETES BY INTRATHYMIC IL-4

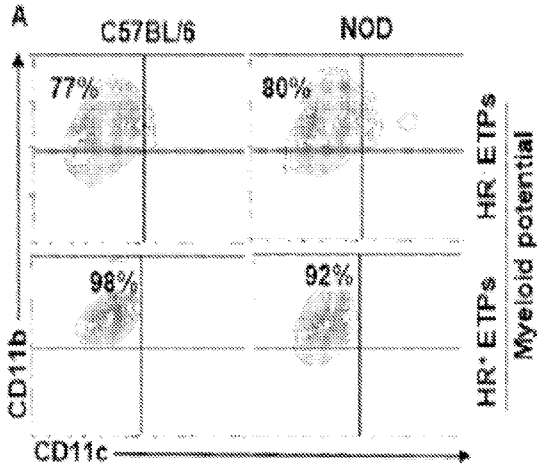

FIG. 1A

(57) Abstract: A treatment composition for the suppression of Type 1 Diabetes (T1D) is described herein, as are methods for using the treatment. Interleukin-4 administrated intrathymically promotes improved central tolerance and minimizes the escape of self-reactive T cells. As a result, negative selection of self-reactive T cells is improved and preservation of a diverse T cell repertoire in the periphery is made possible in patients with or susceptible to T1D.

WO 2025/035125 A1

SUPPRESSION OF TYPE 1 DIABETES BY INTRATHYMIC IL-4

CROSS-REFERENCE TO RELATED APPLICATION

[0001] This application claims the benefit of U.S. Provisional Patent Application No. 63/531,847, filed August 10, 2023, which is incorporated by reference herein in its entirety.

GOVERNMENT LICENSE RIGHTS

[0002] This invention was made with government support under National Institute of Health (NIH) Grant Nos. R01 DK 093515 and R56 DK115441. The government has certain rights in the invention.

SEQUENCE LISTING

[0003] This application contains a sequence listing, the contents of the electronic sequence listing (UMCO-40491WO-17193-00123.xml; Size: 13,000 bytes; Date of Creation: August 9, 2024) are hereby incorporated by reference in its entirety.

BACKGROUND

[0004] Type 1 diabetes (T1D) is an autoimmune disorder characterized by the destruction of insulin-producing beta cells in the pancreas, leading to insufficient insulin production and dysregulation of blood glucose levels. At its core, T1D can be viewed as a manifestation of T cell dysfunction. In healthy individuals, regulatory T cells play a crucial role in maintaining self-tolerance and preventing autoimmune responses. However, in T1D, there is a breakdown in this regulatory mechanism. Autoreactive or 'self-reactive' T cells escape normal central tolerance processes in the thymus and attack pancreatic cells. This aberrant T cell activity creates an immunological imbalance that ultimately results in T1D.

[0005] Interleukin proteins, a family of cytokines crucial for immune system regulation, have been the focus of a great deal of study of autoimmune disorders like T1D and experimental allergic encephalomyelitis (EAE). Interleukins (IL) mediate communication between immune cells

such as T cells. Specific cytokines IL-4 and IL-13 have gained particular attention in this context given their similar anti-inflammatory function. Both IL-4 and IL-13 comprise a heteroreceptor (HR) which comprises IL-4Rα and IL-13Rα1 chains, and thus, signaling by these cytokines through the HR has been an area of primary focus. Somewhat paradoxically, gene deletion of the HR leads to divergent outcomes in T1D and experimental allergic encephalomyelitis (EAE). HR gene deletion nullifies signaling in IL-4 and IL-13, so the contrasting outcomes observed in T1D and EAE suggest that there are differences in HR function between the non-obese diabetic (NOD) autoimmune model, which is a mouse strain used in the study of T1D, and the C57BL/6 autoimmune model, which is a mouse strain used in the study of EAE. Both differential expression of the HR and signaling disparity through the receptor could account for the functional divergence between the two strains. HR is thus held to play a role in regulation of central tolerance of self-reactive T cells in the NOD model.

[0006] There exists a subset of early thymic progenitors (ETPs) which express the HR. Thus, in the microenvironment of the thymus, IL-4 impacts the fate decision of HR^+ ETPs, ordinarily leading to a fine-tuning of T cell selection and protection against EAE in C57BL/6 mice. However, it is demonstrated herein that unlike C57BL/6 HR^+ ETPs, which invariably give rise to cells of the myeloid lineage such as macrophages and erythrocytes, NOD HR^+ ETPs remain multipotent and can mature into the myeloid or lymphoid lineages, as initially defined in ETPs. Nevertheless, *in vivo*, the NOD HR^+ETPs are restricted to the lymphoid T cell lineage due to inadequate levels of IL-4 cytokine in the thymic microenvironment. Under these circumstances, unlike in C57BL/6 mice, no NOD HR^+ETP-derived dendritic cells (DCs) could develop. DCs play a vital role in central tolerance by eliminating self-reactive T cells in the thymus. Since insufficient IL-4 levels in NOD thymic microenvironments preclude HR^+ETP-derived DC development, thymic negative selection is not heightened, and NOD mice develop spontaneous T1D.

[0007] Thus, described herein are methods of perfecting negative selection of self-reactive T cells and preserving a diverse T cell repertoire in the periphery by intrathymic enrichment with IL-4. Such enrichment is held to enhance the fitness of cytokine signaling through the HR, reversing commitment to the myeloid lineage, and thereby serve as a treatment for suppression of Type 1 Diabetes.

SUMMARY OF THE DISCLOSURE

[0008] The present disclosure overcomes the problems inherent in the art and provides compositions for suppression of Type 1 Diabetes (T1D), methods of making and using such compositions, and methods of administering such compositions for suppression of T1D.

[0009] In one aspect, the present disclosure generally provides an efficacious T1D treatment composition.

[0010] In another aspect, the present disclosure generally provides methods for making and/or producing an efficacious T1D treatment composition.

[0011] In another aspect, the present disclosure generally provides a T1D treatment composition that reduces the severity of or the incidence of T1D.

[0012] In another aspect, the present disclosure generally provides methods for reducing the incidence and/or severity of clinical signs of T1D.

[0013] The treatment composition according to the disclosure may be administered or applied systemically through an intravenous, intravascular, intramuscular, intranasal, intraarterial, intraperitoneal, oral, subcutaneous, transdermal, or intrathecal route. Preferably, the composition is administered or applied orally or intramuscularly. In a particularly suitable embodiment, the composition is administered intrathymically, Depending on the desired duration and effectiveness of the treatment, the compositions according to the disclosure may be administered once or several times, also intermittently, for instance on a daily basis for several days, weeks or months, and in different dosages.

[0014] The compositions of the present disclosure can also comprise the addition of any stabilizing agent, such as for example saccharides, trehalose, mannitol, saccharose and the like, to increase and/or maintain product shelf-life and/or to enhance stability.

[0015] According to a further aspect, at least one cytokine protein is provided in the treatment composition at an inclusion level effective for inducing the desired immune response, namely reducing the incidence of or lessening the severity of clinical signs resulting from T1D.

[0016] Those of skill in the art will understand that the composition herein may incorporate known injectable, physiologically acceptable, sterile solutions. For preparing a ready-to-use solution for parenteral injection or infusion, aqueous isotonic solutions, such as e.g. saline or corresponding plasma protein solutions are readily available. In addition, the treatment compositions of the present disclosure can include diluents, isotonic agents, stabilizers, or adjuvants. Diluents can include water, saline, dextrose, ethanol, glycerol, and the like. Isotonic agents can include sodium chloride, dextrose, mannitol, sorbitol, and lactose, among others. Stabilizers include albumin and alkali salts of ethylenediaminetetraacetic acid, among others. Suitable adjuvants are those described above. Oral forms of the composition are also envisioned, and in some forms, preferred.

[0017] The treatment compositions described herein can further include one or more other immunomodulatory agents such as, e. g., interleukins, interferons, or other cytokines. The treatment compositions can also include Gentamicin.

[0018] Another aspect of the present disclosure relates to a kit. Generally, the kit includes a container comprising at least one dose of the T1D treatment composition as provided in this disclosure.

[0019] A further aspect relates to the use of any of the compositions provided herewith as a medicament, even more preferably as a treatment. Moreover, the present disclosure also relates to the use of any of the compositions described herein, for the preparation of a medicament for lessening the incidence and/or severity of clinical and/or postmortem symptoms or signs associated with T1D. Preferably, the medicament is for the suppression of T1D.

[0020] In the present description, the terms polypeptide, peptide and protein are interchangeable.

[0021] It must be understood that the disclosure does not relate to the polypeptides in natural form, that is to say that they are not taken in their natural environment but that they can be isolated or obtained by purification from natural sources, or else obtained by genetic recombination, or alternatively by chemical synthesis, and that they can thus contain unnatural amino acids.

[0022] It is understood that "suppression" as used in the present disclosure, includes the complete prevention of T1D, but also encompasses a reduction in the severity of or incidence of clinical and/or postmortem signs associated with or caused by T1D. Such suppression is also referred to herein as a protective effect.

[0023] It is understood that for the purposes of the present disclosure, the terms "suppression" and "treatment" are effectively interchangeable.

[0024] The pharmaceutical compositions according to the disclosure will contain an effective quantity of the compounds of the disclosure, that is to say in sufficient quantity of said compound(s) allowing the desired effect to be obtained, such as, for example, the modulation of the clinical signs of T1D. The person skilled in the art will know how to determine this quantity, as a function, for example, of the age and of the weight of the individual to be treated, of the state of advancement of the pathology, of the possible secondary effects and by means of a test of evaluation of the effects obtained on a population range, these tests being known in these fields of application.

[0025] These compounds can be administered by the systemic route, in particular, by the intravenous route, by the intramuscular, intradermal or subcutaneous route, or by the oral route. In a more preferred manner, the treatment composition according to the disclosure will be administered by the intramuscular route, through the food or by nebulization only once, or several times, staggered over time.

[0026] When administered as a liquid, the present treatment may be prepared in the form of an aqueous solution, syrup, an elixir, a tincture and the like. Such formulations are known in the art and are typically prepared by dissolution of the treatment composition and other typical additives in the appropriate carrier or solvent systems. Suitable carriers or solvents include, but are not limited to, water, saline, ethanol, ethylene glycol, glycerol, etc. Typical additives are, for example, certified dyes, flavors, sweeteners and antimicrobial preservatives such as thimerosal (sodium ethylmercurithiosalicylate). Such solutions may be stabilized, for example, by addition of partially hydrolyzed gelatin, sorbitol or cell culture medium, and may be buffered by conventional methods using reagents known in the art, such as sodium hydrogen phosphate,

sodium dihydrogen phosphate, potassium hydrogen phosphate, potassium dihydrogen phosphate, a mixture thereof, and the like.

[0027] Liquid formulations also may include suspensions and emulsions that contain suspending or emulsifying agents in combination with other standard co-formulants. These types of liquid formulations may be prepared by conventional methods. Suspensions, for example, may be prepared using a colloid mill. Emulsions, for example, may be prepared using a homogenizer.

[0028] Parenteral formulations, designed for injection into body fluid systems, require proper isotonicity and pH buffering to the corresponding levels of porcine body fluids. Isotonicity can be appropriately adjusted with sodium chloride and other salts as needed. Suitable solvents, such as ethanol or propylene glycol, can be used to increase the solubility of the ingredients in the formulation and the stability of the liquid preparation. Further additives that can be employed in the present formulation include, but are not limited to, dextrose, conventional antioxidants and conventional chelating agents such as ethylenediamine tetraacetic acid (EDTA). Parenteral dosage forms must also be sterilized prior to use.

[0029] The following examples demonstrate certain aspects of the present disclosure. However, it is to be understood that these examples are for illustration only and do not purport to be wholly definitive as to conditions and scope of this disclosure. It should be appreciated that when typical reaction conditions (e.g., temperature, reaction times, etc.) have been given, the conditions both above and below the specified ranges can also be used, though generally less conveniently. The examples are conducted at room temperature (about 23˚C to about 28˚C) and at atmospheric pressure. All parts and percentages referred to herein are on a weight basis and all temperatures are expressed in degrees centigrade unless otherwise specified. Further unless noted otherwise, all components of the disclosure are understood to be disclosed to cover "comprising", "consisting essentially of", and "consisting of" claim language as those terms are commonly used in patent claims.

[0030] In various forms, the methods of the present disclosure include a method of treatment of an autoimmune disease by increasing a level of IL-4 in a thymus of a patient. The autoimmune disease is T-cell mediated, such as Type 1 diabetes. IL-4 levels can be increased

exogenously, as by direct intrathymic injection of IL-4, or endogenously, such as by stimulating upregulation of IL-4. Upregulation of IL-4 can be performed by any manner known to one of ordinary skill in the art, such as by administration of αGalCer to stimulate cytokine production in iNKT cells. The precise dosage and schedule of administration can vary according to the needs of the patient. For example, IL-4 can be injected into the thymus of a human patient at a dosage level of 200 to 500 units, and can be administered once a month for three months.

BRIEF DESCRIPTION OF THE DRAWINGS

[0031] The following drawings form part of the present specification and are included to further demonstrate certain aspects of the present disclosure. The disclosure may be better understood by reference to one or more of these drawings in combination with the detailed description of specific embodiments presented herein.

[0032] FIGS. 1A and 1B are contour plots illustrating representative experiments showing commitment to myeloid (CD11b/CD11c) and lymphoid (CD25) lineages as measured by flow cytometry. In FIG. 1A, NOD and C57BL/6 HR^+ and HR^- ETPs were sorted from the thymus of either strain and cultured on OP9 cells. In FIG. 1B, NOD and C57BL/6 HR^+ and HR^- ETPs were sorted from the thymus of either strain and cultured on OP9-DL1 cells.

[0033] FIG. 1C shows the number of myeloid (CD11b/CD11c) and lymphoid (CD25) cells, where each bar graph represents the mean ± SD of data compiled from four different experiments.

[0034] FIG. 1D shows contour plots from a representative experiment illustrating commitment of the ETPs to myeloid (CD11b), DC (CD11c), and lymphoid (CD25) lineages at six (D6) and 10 (D10) days of culture. HR^+ ETPs from both NOD and C57BL/6 strains cultured on mixtures of OP9/OP9-DL1 (1:1) stromal cells in the presence of GM-CSF, IL-7, and Flt3.

[0035] FIG. 1E shows the percentage of different cell lineages compiled from four experiments. $***p < 0.001$ as determined by two-tailed, unpaired Student *t* test. HR^+ ETPs from

both NOD and C57BL/6 strains cultured on mixtures of OP9/OP9-DL1 (1:1) stromal cells in the presence of GM-CSF, IL-7, and Flt3.

[0036] FIG. 2A shows representative contour plots for expression of CD11b, CD11c, and CD3 markers. CD45.1 NOD and CD45.2 C57BL/6 HR^+ ETPs were injected intrathymically into CD45.2 NOD and CD45.1 C57BL/6 recipients, respectively. After 16 days, thymi were harvested and HR^+ ETP-derived cells were analyzed for lineage phenotype.

[0037] FIG. 2B shows the frequency of $CD11c^+$ DCs and $CD3^+$ T cells corresponding to the experiment of FIG. 2A.

[0038] FIG. 2C shows a contour plot from a representative experiment for CD4 and CD8 expression on NOD HR^+ ETP-derived T cells as well as a bar graph showing CD4 and CD8 expression results compiled from four experiments.

[0039] FIG. 2D illustrates a representative experiment analyzing expression of other lymphoid lineage phenotypes including Tet^+ iNKT cells and $CD19^+$ B cells. $***p < 0.001$ as determined by two-tailed, unpaired Student *t* test.

[0040] FIG. 3A shows histograms resulting from an experiment in which HR^+ ETPs from C57BL/6 and NO mice were analyzed *ex vivo* for phosphorylation of different isoforms of STAT1 and STAT6 transcription factors. The histograms show a representative experiment, while the bar graphs show results compiled from three experiments.

[0041] FIG. 3B shows bar graphs of mRNA expression for IL-7Rα, Notch1, and CEBP/α in HR^+ ETPs.

[0042] FIGS. 3C and 3D show results from experiments where total thymocytes from 6-8-week-old mice were used. In FIG. 3C, the mice were used to extract RNA. In FIG. 3D, the mice were stimulated with PMA/Ionmycin. mRNA expression was analyzed by RT-PCR while IL-4 and IL-13 secretion was determined by ELISA. Each bar represents data compiled from three experiments. $*p* < 0.05$, $***p < 0.001$ as determined by two-tailed, unpaired Student *t* test.

[0043] FIGS. 3E and 3F show data for cells that stain positive for CD3 and αGlaCer tetramer (iNKT-tet) among fresh CD8 depleted thymocytes. FIG. 3E shows cell percentages while FIG. 3F

shows numbers of cells. ***$p < 0.001$ as determined by two-tailed, unpaired Student *t* test from four experiments.

[0044] FIG. 3G shows contour plots and a bar graph. Contour plots show intracellular IL-4 production sorted by iNKT cells that were stimulated with anti-CD3/anti-CD28. The bar graph shows the number of cells staining for intracellular IL-4. ***$p < 0.001$ as determined by two-tailed, unpaired Student *t* test from four experiments.

[0045] FIG. 3H shows bar graphs depicting the percentages of different subsets of iNKT cells including iNKT1 ($CD122^+$ $CD4^{+/-}$ $ICOS^-$), iNKT2 ($CD112^-$ $CD4^+$ $ICOS^+$), and iNKT17 ($CD122^-$ $CD4^-$ $ICOS^+$) among all iNKT cells.

[0046] FIG. 3I shows a bar graph depicting the percentage of IL-4 producing iNKT subset among total iNKT cells. The data is compiled from four experiments. *$p < 0.05$, **$p < 0.01$, ***$p < 0.001$ as determined by two-tailed, unpaired Student *t* tests.

[0047] FIG. 4A shows contour plots from a representative experiment illustrating reduction in fate decision towards the T cell lineage. NOD HR^+ ETPs were cultured on OP9-DL1 + IL-7/Flt3 in the absence (NIL) or presence (treated) of IL-4 or IL-13 for 10d.

[0048] FIG. 4B shows bar graphs showing the frequency of lymphoid lineage cells compiled from four experiments. NOD HR^+ ETPs were cultured on OP9-DL1 + IL-7/Flt3 in the absence (NIL) or presence (treated) of IL-4 or IL-13 for 10d.

[0049] FIG. 4C shows histograms showing a representative phosphorylation experiment. The HR^+ ETPs were stimulated with IL-4, IL-13, IL-4 + 13, or NIL (PBS) and phosphorylation of STAT6 and STAT1 transcription factors were analyzed by flow cytometry.

[0050] FIG. 4D shows bar graphs showing MFI data compiled from three experiments. The HR^+ ETPs were stimulated with IL-4, IL-13, IL-4 + 13, or NIL (PBS) and phosphorylation of STAT6 and STAT1 transcription factors were analyzed by flow cytometry.

[0051] FIG. 4E shows contour plots showing a representative experiment illustrating the frequency of $CD25^+$ lymphoid lineage cells and a bar graph showing compiled results from three experiments. Four-week-old IL-13Rα$1^{+/+}$-GFP reporter NOD mice were given intrathymic IL-4

weekly for two weeks. Seven days later, HR^+ ETPs were sorted from the thymi of these mice and cultured on OP9-DL1 stromal cells for 10 days.

[0052] FIG. 4F shows contour plots showing a representative experiment illustrating expression of CD3 on TEP-derived cells and a bar graph representing the average frequency of $CD3^+$ cells as compiled from three different experiments. HR^+ ETPs sorted from CD45.1 IL-13R$\alpha1^{+/+}$-GFP reporter NOD mice were stimulated with IL-4 *ex vivo* and injected intrathymically into a congenic NOD host (CD45.2). On day 16 after transfer, thymic cells were analyzed for lineage commitment.

[0053] FIG. 4G shows contour plots showing a representative experiment illustrating expression of CD11b, CD11c, and CD8α on ETP-derived cells and a bar graph showing the frequency of $CD11b^+CD11c^+$, $CD11b^+$, $CD11c^+$, and $CD11c^+CD8\alpha^+$ cells of data compiled from three experiments. $*p < 0.05$, $**p < 0.01$, $***p < 0.001$ as determined by two-tailed, unpaired Student *t* test. HR^+ ETPs sorted from CD45.1 IL-13R$\alpha1^{+/+}$-GFP reporter NOD mice were stimulated with IL-4 *ex vivo* and injected intrathymically into a congenic NOD host (CD45.2). On day 16 after transfer, thymic cells were analyzed for lineage commitment.

[0054] FIG. 5A shows a schematic representation of the animal model used to determine the effect of IL-4 on negative selection of T cells. In this model, NOD HR^+ETPs (50×10^3) were treated with IL-4 *ex vivo* and injected intrathymically (i.t) into NOD MHC I^-II^- mice. Two weeks later, the hosts were given i.t positively selected $CD69^+$ double positive ($CD4^+CD8^+$) thymocytes from MHC I^+II^+ congenic (CD45.2) mice. After two weeks, thymi were harvested and analyzed for live CD4 and CD8 single positive T cells.

[0055] FIG. 5B shows the total number of CD4 (left) and CD8 (right) single positive $CD3^+$ T cells from the model of FIG. 5A.

[0056] FIG. 5C shows the percentage of donor T cells undergoing apoptosis (7-AAD) and expressing Nur77, a marker for negative selection in the model of FIG. 5A. $*p < 0.05$, $**p < 0.01$ as determined by two-tailed, unpaired Student *t* test from three experiments.

[0057] FIG. 5D shows dot plots depicting representative experiments for tetramer staining obtained with pooled sample from two pancreases and a graph. 4-week-old NOD mice were

injected intrathymically with PBS (NIL) or with IL-4 once a week for two weeks. At 12 weeks of age, pancreatic T cells were analyzed for the frequency of CD4 T cells that stain positively with insulin-specific tetramers. The graph shows the mean percentage ± SEM obtained from 9 to 10 samples. $^{**}p < 0.01$ as determined by two-tailed, unpaired Student *t* test.

[0058] FIG. 5E shows a graph illustrating the percentage of diabetic mice in a model in which mice were injected with either diluent or IL-4. 4-week-old NOD mice were given i.t IL-4 once a week for two weeks and then monitored for blood glucose level (BGL) starting at 12 weeks of age. $^{**}p < 0.01$ as determined by Mann-Whitney *U* test.

[0059] FIG. 6A shows 2D heat maps of the relative frequency of V and J segments of TCRβ chain. V-J heat maps from the SP (top panels) and PLN (bottom panels) are illustrated. Four-week-old NOD mice (4 per group) were treated with intrathymic IL-4 or PBS once per week for two weeks. At 9 weeks of age prior to disease onset, the SP and PLN were harvested and used to sort $TCR\beta^+$ T cells. RNA isolated from T cells was utilized to generate cDNA libraries and the variable region of the TCRβ chain was sequenced.

[0060] FIG. 6B shows bar graphs showing the frequency of Vβ13 usage in IL-4 versus PBS treated mice from SP and PLN T cells in the experiment of FIG. 6A.

[0061] FIG. 6C shows bar graphs showing the frequency of a particular CDR3 length among total number of CDR3s. CDR3s were normalized such that each unique CDR3 is equal to a count of 1, regardless of the total number of identical CDR3s. Individual CDR3s were grouped on the basis of nucleotide numbers (length).

[0062] FIG. 6D shows the percentage of T cells with CDR3 encompassing different ranges of 'N' additions.

[0063] FIG. 6E shows the frequency of the 10 most frequent CDR3s among the total number of CDR3 sequences read.

[0064] FIG. 7A shows 2D heat maps of the relative frequency of V (y-axis) and J (x-axis) segments of TCRβ chain. V-J heat maps from the SP (top panels) and PLN (bottom panels) are illustrated. Four-week-old NOD mice (4 per group) were treated with intrathymic IL-4 or PBS once

per week for two weeks. At the onset of diabetes (12 weeks of age), the SP and PLN were harvested and used to sort TCRβ$^+$ T cells. RNA isolated from T cells was utilized to generate cDNA libraries and the nucleotide sequence of variable region of the TCRβ chain was determined.

[0065] FIB. 7B shows the percentage of Vβ13 usage in IL-4 versus PBS treated mice from SP and PLN T cells from the experiment of FIG. 7A.

[0066] FIG. 7C shows the percentage of different Vβ reads that have undergone a range of nucleotide trimming in comparison to their parental germline genes from the experiment of FIG. 7A.

[0067] FIG. 7D shows the percentage of different CDR3 reads with a range of 'N' additions from the experiment of FIG. 7A.

[0068] FIG. 7E shows the percentage of different short (27-36) and long (37-45) CDR3 reads among IL-4 treated and untreated mice from the experiment of FIG. 7A.

[0069] FIG. 8A shows contour plots resulting from an exemplary study in which thymic cells from NOD IL-13Rα1-GFP reporter mice were depleted of Lin$^+$ cells, and Lin$^-$CD4$^-$CD8$^-$ cells were analyzed for CD25 and CD44 expression. CD25$^-$CD44$^+$ cells (DN1 cells) were further assessed for c-Kit and CD24 expression to distinguish the different subsets within the DN1 population. The left contour plot shows the different DN1 subsets on the basis of expression of CD24$^+$c-Kit^{hi} (DN1a,b), CD24$^+$c-Kit^{int} (DN1c), CD24$^+$c-Kit$^-$ (DN1d), and CD24$^-$c-Kit$^-$ (DN1e). The right contour plots show expression of IL-13Rα1 (HR) on the different subsets.

[0070] FIG. 8B shows HR expression data on the different subsets compiled from four experiments from the study of FIG. 8A. ***$p < 0.001$ as determined by two-tailed, unpaired Student *t* test.

[0071] FIG. 9A shows surface HR expression data compiled from 5 experiments wherein HR$^+$ ETPs from C57BL/6 and NOD mice were analyzed for receptors expression by both flow cytometry and RT-PCR. *$p < 0.05$ as determined by two-tailed, unpaired Student *t* test.

[0072] FIG. 9B shows IL-13Rα1 gene expression from the study of FIG. 9A. **$p < 0.01$ as determined by two-tailed, unpaired Student *t* test.

[0073] FIG. 9C shows IL-4Rα1 gene expression from the study of FIG. 9A. $**p < 0.01$ as determined by two-tailed, unpaired Student *t* test.

[0074] FIG. 9D shows IL-13Rα2 gene expression from the study of FIG. 9A. $**p < 0.01$ as determined by two-tailed, unpaired Student *t* test.

[0075] FIG. 10A shows the frequency of SIRPα$^-$ CD11c$^+$CD8$^+$ thymic resident DCs from C57BL/6 relative to NOD mice, as determined from an exemplary study in which CD3$^-$ thymocytes from C57BL/6 and NOD mice were stained for CD11b, CD11c, CD8, and SIRPα at the age of 6-8 weeks and 12-14 weeks. $**p < 0.01$ as determined by two-tailed, unpaired Student *t* test from five experiments.

[0076] FIG. 10B shows a comparison of the frequency of SIRPα$^-$CD11c$^+$CD8$^+$ thymic resident DCs among 6-8 week versus 12-14 week old NOD mice from the exemplary study of FIG. 9A. $**p < 0.01$ as determined by two-tailed, unpaired Student *t* test from five experiments.

[0077] FIG. 11 shows a diagrammatic comparison of the effects of intrathymic IL-4 on exemplary healthy mice and exemplary diabetic mice as described herein.

DETAILED DESCRIPTION

[0078] The following detailed description and examples set forth preferred materials and procedures used in accordance with the present disclosure. It is to be understood, however, that this description and these examples are provided by way of illustration only, and nothing therein shall be deemed to be a limitation upon the overall scope of the present disclosure.

[0079] "A", "an", and "the" include the singular and plural forms thereof unless the context clearly indicates otherwise.

[0080] "Comprising", "comprises", "comprise", "including", "includes", "include", "having", "has", and "with" are all defined as being inclusive of the specified components as well as other unspecified components and can be used interchangeably.

[0081] HR$^+$ ETPs, whether from NOD or C57BL/6 mice, remain multipotent like other subsets of ETPs. *In vivo* fate decision analysis shows that C57BL/6 HR$^+$ ETPs are restricted to the myeloid lineage while NOD HR$^+$ ETPs commit only to the T cell lineage. These findings are

supported by differential STAT activation patterns and selective expression of lineage-specific developmental transcription factors. Indeed, differentiating C57BL/6 HR^+ ETPs display upregulation of both STAT 1 and STAT6 phosphorylation, but downregulation of Notch 1 T cell lineage developmental transcription factor, while developing NOD HR^+ ETPs have minimal STAT phosphorylation but display significant Notch 1 upregulation. As IL-4 and IL- 13 are known to signal through the HR, the differential fate decision in the two strains reported here coincides with a disparity in cytokine expression in the thymic microenvironment. Two logical questions arose from these observations and these include: the root cause for diminished IL-4 in NOD mice and how IL-4 reduction accounts for the differential fate decision in the two strains. Given that the two strains are known to exhibit discrepancies in the frequency of NKT cells and subsets of this population produce IL-4 in the thymus, the frequency of thymic iNKT cells and their ability to produce IL-4 was analyzed. Interestingly, the frequency of INKT cells in the thymus of NOD mice was significantly reduced relative to C57BL/6 and this lead to diminished IL-4 production.

[0082] More importantly, the frequency of iNKT2 cells is reduced in the NOD relative to CS7BL/6 and this is likely responsible for the overall reduction in IL-4 production which coincides with a negative feedback loop between ETP-derived myeloid cells and IL-4-producing iNKT cells.

[0083] As for the effect of IL-4 on ETP fate decision, one notes that the HR^+ ETPs from the two strains had disparities in STAT signaling, likely suggesting that IL-4 does not serve as an ON/OFF switch of the HR. Rather, the magnitude of the cytokine dictates its fitness in STAT signaling and thus HR^+ ETP fate decision. While structural features can influence cytokine and receptor interactions, the findings here uncover yet another parameter whereby the level of IL-4 in the thymic microenvironment influences its signaling fitness and thus commitment of ETPs to specific cell lineages. This previously unrecognized attribute positions IL-4 cytokine in the forefront for fine-tuning of T cell selection, adjustment of lymphocyte repertoire diversity, and manifestation of autoimmunity. Indeed, low levels of IL-4 sustains ETP commitment to T cells, but i.t. enrichment raises IL-4 to optimal levels that block ETP commitment to T cells and enable the development of $CD11c^+CD8\alpha^+$ DCs. Bone marrow-derived $CDl1c^+CD8\alpha^+$ DCs migrate to the thymus and participate in negative T cell selection. ETP-derived $CD1lc^+CD8\alpha^+$ DCs also contribute to negative selection of self-reactive T cells. Moreover, there is restoration of repertoire diversity

which could not be due to blockade of ETP fate decision to T cells or negative selection of self-reactive T cells but rather to usage of alternative V-D-J combinations. Although these findings bode well with non-defective rather than compromised T cell selection, they point to IL-4 as an uneven two-edged sword in that low levels restrict TCR diversity with short CDR3s and higher levels engender diverse repertoire with limited V-trimming and longer CDR3s.

[0084] In various embodiments, the treatment method described herein comprises increasing IL-4 levels in the thymus of a patient that has been diagnosed with an autoimmune disease. The Examples provided below describe Type 1 diabetes as an exemplary autoimmune disease; however, the method of increasing thymic IL-4 levels described herein has the ultimate effect of promoting central tolerance, improving peripheral tolerance and cultivating a healthier T cell repertoire, and will thereby function to suppress any T-cell-mediated autoimmune disease. Additionally, although the examples provided below describe increasing the levels of IL-4 in a patient's thymus via direct intrathymic injection, any method known to one of ordinary skill for increasing IL-4 levels in the thymus is considered to be within the scope of the described methods. For example, any technique known to upregulate IL-4 production, such as the administration of the iNKT cell antigen α-galactosylceramide, is also considered to be within the scope of the methods described herein.

[0085] The intrathymic injection of IL-4 into a patient for the treatment of an autoimmune disease, as described herein, can be administered with dosages and frequency according to the needs of the patient and the understanding of one of ordinary skill in the art. Thus, for an exemplary human patient, dosages of IL-4 can range from 200 to 500 units, from 250 to 450 units, from 300 to 400 units, or from 325 to 375 units. As used here, a unit is an amount of a biologically active agent (such as a drug or antigen) required to produce a specific result under strictly controlled conditions. A dose of IL-4 can be injected i.t. once a month, twice a month, or more, for one, two, three, four, or more months, and/or until the clinical signs of the autoimmune disease are deemed to be adequately suppressed.

[0086] Overall, IL-4, which is usually produced as a consequence of parasitic infection or in response to allergens, has always been associated with peripheral tolerance, the findings here

though extend its functions to central tolerance, as well as calibration of the T cell repertoire and illuminate the link between iNKT cells and T1D.

EXAMPLES

[0087] The following examples illustrate embodiments of the disclosure. Nothing in these examples should be limiting to the disclosure as these are representative in nature.

EXAMPLE 1

Methods

[0088] **Mice.** All animal experiments were done according to protocols approved by the University of Missouri Animal Care and Use Committee. CD45.1 and CD45.2 C57BL/6 and NOD as well as NOD MHC $I^{-/-}II^{-/-}$ mice were purchased from The Jackson Laboratory (Bar Harbor, ME). IL-13Rα1$^{+/+}$-GFP C57BL/6 mice were previously described. The IL-13Rα1$^{+/+}$-GFP NOD mice were generated by breeding IL-13Rα1$^{+/+}$-GFP C57BL/6 mice onto the NOD background via speed congenic technology based on 58 microsatellite markers on sequences between the C57BL/6 donor strain and NOD recipient strain. A total of eight backcrosses with wild-type NOD mice were performed to ensure homozygosity of NOD alleles. Only 6-8 week old female mice were used throughout the study unless otherwise noted. All animals were maintained under specific pathogen-free conditions in individually ventilated cages and kept on a 12 h light-dark cycle with access to food and water ad libitum.

[0089] **Flow Cytometry: Tetramers.** PBS57-CD1d, synthetic α-galactosylceramide (αGalCer) loaded onto CD1d molecules was obtained from the National Institutes of Health Tetramer Core Facility.

[0090] **Flow Cytometry: Antibodies.** Anti-IL-4 (11B11), anti-CD3 (145-2C11), anti-CD4 (RM4-5), anti-CD8 (53-6.7), anti-CD11b (M1/70), anti-CD11c (HL3), anti-CD25 (7D4), anti-CD44 (IM7), anti-CD45 (30-F 11), anti-CD45.1 (A20), anti-CD 117 (2B8) were purchased from BD Biosciences (San Jose, CA). Anti-CD45.2 (104) was purchased from eBioscience (San Diego, CA). Anti-ICOS (C398.4A), anti-TCRβ (H57-597), anti-CD122 (TMβ1) were purchased from Biolegend (San Diego, CA).

[0091] **Flow Cytometry: Lineage (Lin) depletion antibodies.** Depleting antibodies were purchased from Miltenyi Biotech (San Diego, CA) as a kit that includes antibodies against CD8α (Ly-2), CD11b (Mac-1), CD11c, CD19, B220 (CD45R), CD49b (DX5), CD105, MHCII$^+$, Ter-119$^+$, and TCRγ/δ. Anti-CD4 microbead antibody (L3T4) was also used in the lineage depletion experiments.

[0092] **Flow Cytometry: Fluorochromes.** Antibodies were directly conjugated to fluorescein isothiocyanate (FITC), phycoerythrin (PE), PE-Cy5, PE-Cy5.5, peridinin-chlorophyll-protein complex (PerCP)-Cy5.5, PE-Cy7, allophycocyanin, allophycocyanin-Cy7 (or allophycocyanin eFluor780), or biotin. Biotinylated antibodies were revealed with Streptavidin PE or allophycocyanin.

[0093] **Flow Cytometry: Sample Reading.** Sample reading wused a BeckMan Coulter CyAn (Brea, CA). Data were analyzed using FlowJo version 10 (Tree Star). Dead cells were excluded using 7-aminoactinomycin D (7AAD; EMD Biosciences).

[0094] **Cell Sorting.** Cell sorting was performed on a Beckman Coulter MoFlo XDP (Brea, CA) cell sorter. Cell purity was routinely checked, and only sorts with a purity of >95% were used.

[0095] **ETPs**. In brief, thymi were harvested from either IL-13Rα1$^{+/+}$-GFP NO or IL-13Rα1$^{+/+}$-GFP C57BL/6 mice after perfusion with PBS, and the CD4$^+$ cells were eliminated by MACS using anti-CD4 microbeads. The ETPs were then isolated after depletion of lineage positive (Lin$^+$) thymic cells. HR$^+$ ETPs (cKit$^+$CD44$^+$CD25$^-$GFP$^+$) were sorted from lineage negative (Lin$^-$) thymic cells of IL-13Rα1$^{+/+}$-GFP reporter mice on the basis of GFP (IL-13Rα1) expression. HR$^+$ ETPs represent the GFP$^+$ cells, and HR$^-$ ETPs represent the GFP$^-$ cells of the lin$^-$cKit$^+$CD44$^+$CD25$^-$ thymic cells.

[0096] **Aβ T cells.** SP and PLN αβ T cells were sorted using anti-TCRβ chain antibody (H57-597), resuspended in RNAprotect Cell Reagent (Qiagen) and shipped to iRepertoire on dry ice.

[0097] **OP9 and OP9-DL1 cell culture.** Briefly, OP9 and OP9-DL1 stromal cells were plated 2 days before initiation of cultures at a concentration of 20,000 cells/mL in 24-well plates. Progenitors were added at 3,000 per well. IL-7 was used at a final concentration of 1 ng/mL (5U), Flt3 ligand (Flt3L) was used at 5 ng/mL (5U). GM-CSF (200U) and IL-4 (5U) (SEQ ID NO:13) were used at 10 ng/mL, and IL-13 (5U) was used at 20 ng/mL. Under these conditions, the lymphoid progeny was most evident at day 10 of OP9-DL1 cell culture and myeloid progeny was evident as

early as day 3 of OP9 cell culture. Cultures using a mixture of OP9/OP9-DL1 stromal cells (1:1) were preformed under similar conditions.

[0098] **Intrathymic Injections.** The cytokine (75U/mouse) was diluted in 30 µL saline and injected into isoflurane-anesthetized mice through the skin between the 3rd and 4th rib of the thoracic cavity using a 0.3-mL, 31-gauge, 8-mm insulin syringe. Cells (5 x 10^4 /mouse) were resuspended in saline and injected in a similar manner as with IL-4.

[0099] **Measurement of STAT activation.** STAT phosphorylation in ETPs was analyzed with or without treatment with cytokines. IL-4 (10U), IL-13 (10U), and IL-4 + IL-13 (10U each) were used during a 3 hour stimulation and excess of cytokines was washed out from the culture. Cells were then fixed, permeabilized, and activation of STAT1 (S727), STAT1 (S701), or STAT6 (Y641) was measured by flow cytometry.

[0100] **RT-PCR.** RNA was isolated from ETPs or total thymic cells by Trizol extraction and isopropanol precipitation. RT-PCR was performed on a StepOnePlus Instrument cycler using Power SYBR Green RNA-to-C_T 1-Step Kit (Applied Biosystems) according to the manufacturer's instructions. RT-PCR was done with primers specific for: GAPDH (Sense 5'-AACTTTGGCATTGTGGAAGG-3' (SEQ ID NO:1); Antisense 5'-GGATGCAGGGATGATGTTCT-3' (SEQ ID NO:2)), C/EBPα (Sense 5'-AGCAACGAGTACCGGGTACG-3' (SEQ ID NO:3), Antisense 5'-GTTTGGCTTTATCTCGGCTC-3' (SEQ ID NO:4)), Notch1 (Sense 5'-GGACATGCAGAACAACAAGG-3' (SEQ ID NO:5), Antisense 5'-CAGTCTCATAGCTGCCCTCA-3' (SEQ ID NO:6)), IL-7Rα (Sense 5'-AGTCCGATCCATTCCCCATAA-3' (SEQ ID NO:7), Antisense 5'-ATTCTTGGGTTCTGGAGTTTCG-3' (SEQ ID NO:8)), IL-4 (Sense 5 '-GGAGATGGATGTGCCAAACG-3' (SEQ ID NO:9), Antisense 5 '-GCACCTTGGAAGCCCTAC-3' (SEQ ID NO:10)), and IL-13 (Sense 5 '-GTGTCTCTCCCTCTGACCCT-3' (SEQ ID NO:11), Antisense 5'-GGGGAGTCTGGTCTTGTGTG-3' (SEQ ID NO:12)). Relative transcript abundance was determined by using the comparative threshold cycle method using the StepOne software (Applied Biosystems) normalization with GAPDH. All samples were run in triplicate.

[0101] **ELISA.** IL-4 and IL-13 production in supernatant was measured using anti-cytokine antibodies from BD Biosciences (San Jose, CA), according to manufacturer instructions. The OD450 was read on a SpectraMax 190 counter (Molecular Devices, Sunnyvale, CA) and analyzed using Softmax Pro 3.1.1 software. Cytokine concentrations were then extrapolated from the

linear portion of a standard curve generated by graded amounts of the respective recombinant cytokine.

[0102] Detection of IL-4/IL-13 production in thymic cells. Thymic cells from C57BL/6 and NOD mice were stimulated with PMA and ionomycin for 6 hours and the supernatant was used to measure cytokines by ELISA as indicated above.

[0103] Detection of IL-4/IL-13 production in iNKT cells. Thymic cells were first stained with allophycocyanin-labeled PBS57-CD1d1 tetramer (iNKT-tet). After extensive washing, the iNKT cells were isolated using anti-allophycocyanin Miltenyi microbeads according to the manufacturer's instructions. Subsequently, the purified iNKT cells were stimulated for 72 hours with anti-CD3 (10 μg/mL) and anti-CD28 (1 μg/mL). Two hours prior to sample analysis, BFA (10 μg/mL) was added to the culture to enhance cytokine retention in the cytoplasm. IL-4 was then measured by intracellular staining.

[0104] Thymic negative selection assay. NOD MHC $I^{-/-}$ $II^{-/-}$ mice were given (i.t.) HR^{+} ETPs (12 x 10^3 cells/mouse) that were pre-treated with IL-4 (5U) for three hours. Two weeks later, the host mice were given positively selected ($CD45.2^{+}/CD69^{+}$) double positive (DP) $CD4^{+}CD8^{+}$ thymocytes. After two weeks, negative T cell selection was measured by determining the number of single positive (SP) T cells as well as by assessing DP cells that are undergoing TCR-mediated apoptosis ($7AAD^{+}$ $Nur77^{+}$).

[0105] Sequencing of the αβ T cell repertoire. Sorted $TCR\beta^{+}$ cells (2 x 10^5 cells per sample) were resuspended in RNAprotect Cell Reagent (Qiagen) and shipped overnight to iRepertoire, Inc. RNA isolation used an RNeasy Mini Kit (Qiagen). Multiplexed cDNA Libraries were created by iRepertoire using nested primers for different variable and constant portions of the TCRβ chain was sequenced at a read depth of 1 million per library. Sequencing was done on the Illumina Miseq system. Each sample included SP or PLN T cells pooled from 4 mice.

[0106] Statistical Analysis. Data were analyzed using either an unpaired, two-tailed Students t-test or Mann-Whitney U test as indicated. All statistical analyses were performed using Prism software version 4.0c (GraphPad).

Example 2

[0107] NOD HR$^+$ ETP fate decision is biased towards the T cell lineage. A new subset of early thymic progenitors (ETPs) was discovered whose potential was restricted to the myeloid lineage. Expression of the IL-4/IL- 13 heteroreceptor (HR) by these ETPs enables the cytokines to inhibit their T cell potential and sustain commitment to the myeloid lineage. Surprisingly, HR expressing ETPs (HR$^+$ETPs) from NOD mice, contrary to C57BL/6 HR$^+$ETPs, remain multipotent and commit to both myeloid and lymphoid lineages (FIGS. 1A-1E). Indeed, culture on OP9 stromal cells shows that both types of ETPs commit to the myeloid lineage (FIG. 1A). However, when the ETPs were cultured on OP9-DL1 stromal cells, the NOD, but not the CS7BL/6, HR$^+$ETPs gave rise to T cells (FIG. 1B). Compiled data from several experiments confirms the flexible fate decision of NOD versus C57BL/6 HR$^+$ETPs (FIG. 1C). In addition, when both types of HR$^+$ETPs were co-cultured on OP9 and OP9-DL 1 cells, the flexible fate decision of NOD versus C57BL/6 HR$^+$ETPs remained active (FIG. 1D) and there were both lymphoid and myeloid cells as demonstrated in data compiled from several experiments (FIG. 1E). These findings are surprising because NOD HR$^+$ETPs belong to the DN1c population (FIG. 8A), a phenotype similar to C57BL/6 HR$^+$ETPs. To ensure that the fate decision flexibility of NOD HR$^+$ETPs observed with the *in vitro* culture system is biologically relevant, an allogenic transfer model was developed and used to assess HR$^+$ ETP maturation *in vivo*. Surprisingly, the NOD HR$^+$ETPs lost their fate decision flexibility like C57BL/6 mice and gave rise to T cells instead of myeloid cells (FIGS. 2A-2D). Indeed, upon intrathymic (i.t) transfer of HR$^+$ETPs into CD45 allogenic hosts the NOD cells yielded only T cells while C57BL/6 differentiated into myeloid cells, including CD11b$^+$ monocytes/macrophages and CD11c$^+$ DCs (FIG. 2A). These results are statistically significant as shown by data compiled from several experiments (FIG. 2B). The T cell restriction of NOD HR$^+$ETPs is stark as no other lymphoid subsets, such as iNKT cells or B cells, were observed (FIGS. 2C and 2D). Overall, the data indicates that NOD HR$^+$ETPs are restricted to the T cell lineage while C57BL/6 HR$^+$ETPs were confined to myeloid cells.

Example 3

[0108] NOD HR$^+$ETPs display diminished STAT activation due to reduced cytokine availability in the thymic microenvironment. It was previously reported that IL-4 arid IL- 13

utilize the HR to induce signal activation of STAT 1 and STAT6 transcription factors, which enable commitment of C57BL/6 ETPs to the myeloid lineage. Since NOD HR$^+$ETPs commit instead to the T cell lineage (FIGS. 2A-2D), it was necessary to determine whether phosphorylation of STAT molecules is compromised in the thymic microenvironment. To this end, HR$^+$ETPs were sorted from both C57BL/6 and NOD mice and assessed *ex vivo* for STAT phosphorylation. The results show that, while STAT1$_{(S727)}$ activation was similar in both strains, phosphorylation of STAT1$_{(S701)}$ and STAT6$_{(Y641)}$ were reduced in NOD HR$^+$ ETPs in comparison to their C57BL/6 counterparts (FIG. 3A). Data compiled from several experiments demonstrates that diminished activation of STAT molecules is statistically significant (FIG. 3A, bar graphs). The diminished STAT phosphorylation in NOD HR$^+$ETPs is accompanied by up regulation of IL-7Rα and Notch 1 transcription factor, both of which serve as markers for commitment to the T cell lineage (FIG. 3B). Furthermore, there was down regulation of CEBP/α, a transcription factor associated with commitment to the myeloid lineage (FIG. 3B). Overall, the differential signaling through the HR and its consequence on ETP fate decisions could be related to lower HR expression on NOD ETPs. This was not, however, the case as NOD ETPs had elevated expression of the HR relative to C57BL/6 ETPs (FIG. 9A) which seemed to correlate with higher expression of IL-13Rα1 (FIG. 9B) rather than IL-4Rα (FIG. 9C). Since IL-13Rα2 expression is similar in both strains (FIG. 9D), it is unlikely that this chain diverts IL- 13Rα1 into a decoy receptor. These observations suggest that IL-4/IL-13 signaling through the HR does not function as an ON/OFF switch but perhaps operates in a rather adaptable fashion. Lower amounts of cytokine in the thymic microenvironment may account for the differential signaling. Indeed, the results show that IL-4 mRNA levels in the NOD thymus were significantly reduced compared to age-matched C57BL/6 samples (FIG. 3C). More strikingly, there was less IL-4 and IL- 13 protein in the NOD compared to C57BL/6 thymus upon stimulation with PMA/Ionomycin (FIG. 3D). Given that IL-13 mRNA levels were similar in both strains and IL-13 protein level was only slightly reduced in the NOD thymus, it may be that the reduction of IL-4 is responsible for differential signaling in NOD HR$^+$ETPs. It has previously been shown that iNKT cells serve as the primary source of IL-4 in the thymus. It is thus logical to envision iNKT cells as the culprit for reduced IL-4 in the thymic environment. To test this premise, the frequency of iNKT cells in the thymus was determined using CD1d:αGlaCer tetramer staining. The findings indicate

that both the percentage (FIG. 3E) and the absolute number (FIG. 3F) of iNKT-tet cells were significantly reduced in the NOD compared to the C57BL/6 thymus. Intracellular cytokine staining shows that the percentage and the absolute number of IL-4-producing iNKT cells are significantly reduced in the NOD versus C57BL/6 mice (FIG. 3G). iNKT cells comprise subsets with signature cytokines, reminiscent of T helper cells, in that iNKT1 produce INF7, iNKT2 produce IL-4, and iNKT 17 produce IL- 17. Enumeration of these subsets indicates that the frequency of iNKT2 cells is reduced in NOD relative to C57BL/6 mice, while iNKT1 and iNKT17 are rather increased in the NOD mice (FIG. 3H). Furthermore, the reduction in the frequency of iNKT2 cells parallels with diminished percentage of IL-4 producing iNKT2 cells (FIG. 3I). Together these results indicate that the reduced microenvironmental IL-4, which is responsible for reversal of signaling and fate decision, is due to a diminished number of iNKT2 cells in the NOD mouse.

Example 4

[0109] Enrichment with IL-4 enables STAT signaling that redirects HR$^+$ETPs fate decision towards myeloid cells. NOD HR$^+$ETPs ultimately give rise to T cells (FIG. 1D). However, upon treatment with IL-4 or IL-13, the T cell lineage potential of HR$^+$ETPs is diminished (FIG. 4A). Data compiled from several experiments indicates that the diminished T cell lineage fate decision of ETPs is statistically significant relative to cells that were not treated with cytokines (FIG. 4B). Note that IL-4 seems to have a more pronounced effect on ETP T cell lineage fate decision, in comparison to IL- 13 (FIGS. 4A-4G). Also, the cytokines affect the signaling in ETPs as IL-4 restores activation of both STAT6 and STAT1, while IL-13 restores only STAT1 phosphorylation (FIG. 4C). The combination of IL-4 and IL- 13 had similar STAT activation pattern as IL-4 alone (FIG. 4C). Compiled data from several experiments demonstrates that the cytokines effects are statistically significant (FIG. 4D). The lack of STAT6 activation by IL-13 (FIGS. 4C and D) may explain the diminished reversal of fate decision observed *in vitro* (FIGS. 4A and 4B). Overall, cytokine-induced STAT activation parallels with fate decision and indicates that NOD HR$^+$ETPs are susceptible to cytokine stimulation and shifting of lineage commitment away from the T cell lineage. As IL-4 seems to drive a more pronounced effect on ETPs maturation, it was used to test its function *in vivo*. Indeed, when cultured *in vitro* on OP9-DL1 cells, HR$^+$ETPs from NOD mice recipient of IL-4

(i.t.) display diminished T cell lineage potential, relative to NIL control (FIG. 4E, left panel). The loss of T cell potential by i.t. IL-4 is statistically significant (FIG. 4E, right panel). Furthermore, when HR^+ETPs are exposed to IL-4 *in vitro* and then transferred i.t. into CD45 allogenic hosts, the T cell potential is again dramatically reduced (FIG. 4F, left panel). Data from several experiments indicates that the T cell potential reduction relative to HR^+ETPs that were not exposed to IL-4 is statistically significant (FIG. 4F, right panel). Interestingly, the loss of T cell potential in IL-4 exposed HR^+ETPs results in a shift into myeloid cells of monocyte/macrophage and DC phenotypes (FIG. 4G, left panel). An important percentage of the $CD11c^+$ DCs belong to the $CD11c^+CD8\alpha^+$ subset. These results are statistically significant as indicated by data compiled from several experiments (FIG. 4G, right panel). Together these findings indicate that enrichment with IL-4 diminishes HR^+ETP T cell potential and yields maturation to myeloid cells and DCs, most of which are $CD11c^+CD8\alpha^+$ cells.

Example 5

[0110] Intrathymic IL-4 sustains HR^+ETP maturation towards antigen presenting cells able to restore negative selection of self-reactive T cells and protect against T1D. FIGS. 4A-4G indicate that intrathymic IL-4 prompts HR^+ETPs to give rise to DCs with substantial fraction belonging to the $CD11c^+CD8\alpha^+$ subset. Since DCs, specifically the $CD11c^+CD8\alpha^+$ subset, play a major role in negative selection of T cells, it was necessary to determine whether IL-4-induced ETP-derived DCs would play a role in selection of self-reactive T cells. An experimental model was then devised to test the contribution of HR^+ETP-derived DCs to selection of self-reactive T cells (FIG. 5A). Accordingly, HR^+ETPs from MHC $I^{+/+}II^{+/+}$ NOD mice were briefly stimulated with IL-4 and then injected (i.t.) into MHC $I^{-/-}II^{-/-}$ NOD hosts. Two weeks later, the mice were given (i.t.) positively selected $CD69^+$ DP ($CD4^+CD8^+$) polyclonal thymocytes to serve as targets for negative selection by the ETP-derived DCs. The results show that mice recipients of IL-4-treated ETP-derived DCs had significantly fewer thymic single positive $CD4^+$ T cells as compared to control mice recipients of HR^+ETPs that were not treated with IL-4 (FIG. 5B, left panel). Similarly, there were also diminished single positive $CD8^+$ T cells relative to the control mice (FIG. 5B, right panel). Moreover, when the residual double-positive (DP) cells were gated out, and the total ($CD4^+$ and

CD8$^+$) single positive (SP) cells were stained for Nur77 and 7AAD, there were significantly more cells dying (7AAD$^+$) by TCR-mediated apoptosis (Nur77$^+$) in the mice recipients of the IL-4-treated ETPs, relative to control mice recipients of ETPs that were not treated with IL-4 (FIG. 5C). These results suggest that IL-4-treated ETPs yielded DCs, especially CD11c$^+$CD8α$^+$ cells, that are known to sustain negative selection of self-reactive T cells. This interpretation bodes well with the observations showing that the frequency of CD8α$^+$CD11c$^+$ DCs was significantly reduced in NOD relative to C57BL/6 mice, both at young and older age (FIGS. 10A and 10B).

[0111] 4-week-old NOD mice were also injected intrathymically with either PBS diluent or with just IL-4, and not with HR$^+$ ETPs, resulting in the data shown in FIGS. 5D and 5E. Treatment with direct IL-4 injection once a week for two weeks resulted in a nearly 10-fold decrease in the frequency of CD4 T cells found during analysis of the pancreatic T cells (FIG. 5D).Strikingly, the impact of IL-4 on T cell selection translates into resistance to the development of diabetes (FIG. 5E). Indeed, NOD mice recipient of intrathymic IL-4 had significantly delayed onset of T1D, relative to control mice given saline instead of IL-4 (FIG. 5E). Overall, intrathymic IL-4 diverts HR$^+$ETP maturation from T cells to DCs able to augment negative selection of self-reactive T cells, leading to protection against T1D.

Example 6

[0112] **Intrathymic IL-4 influences the diversity and the dynamics of the peripheral lymphocyte repertoire.** IL-4 biases ETP fate decision from T cells to myeloid cells that are able to function as APCs and impact negative selection of self-reactive T cells (FIGS. 4A-4G and FIGS. 5A-5E). Under these circumstances, it is likely that the thymic output seeds the periphery with a divergent lymphocyte repertoire. To test this premise, splenic (SP) and pancreatic lymph node (PLN) TCR β$^+$ lymphocytes were isolated from mice recipient of i.t. IL-4 prior to (9 weeks of age) and during the onset (12 weeks of age) of T1D and their Vβ chain nucleotide sequences were determined by RNA-Seq. Heat map comparison of Vβ usage among IL-4 recipient and untreated (NIL) mice prior to onset of T1D shows a similar Vβ-Jβ profile in the SP but a distinct pattern in the PLN (FIG. 6A). Notably, many distinct Vβ-Jβ combinations are more frequently used in the PLN of IL-4 recipient mice (FIG. 6A, lower panel). However, the usage of Vβ13 genes (Vβ13-1,

Vβ13-2, and Vβ13-3), which are associated with type one diabetes, is reduced by IL-4 (FIG. 6B). The complementarity-determining region 3 (CDR3) of the TCRβ chain is critical for determining antigen specificity. In T1D patients, T cells have shorter CDR3 regions with fewer random nucleotide insertions than healthy individuals matched for HLA haplotype. Since intrathymic IL-4 confers resistance to T1D, it is likely that it influences the length of the CDR3 region. Profiling of CDR3 length shows that most of the SP T cells from IL-4 treated mice tend to have longer CDR3s than T cells from untreated mice (FIG. 6C, upper panel). This correlates with the more prevalent longer N addition sequences (33% in the 6-10 N addition range) in the IL-4 treated mice (FIG. 6D, upper panel). In the PLN, however, T cells from IL-4 treated mice showed CDR3 length spread throughout a wide spectrum, while those from untreated mice were confined to either short or long range CDR3s (FIG. 6C, lower panel). This is likely related to more prevalent shorter N addition sequences in the IL-4 treated versus untreated mice (FIG. 6D, lower panel).

[0113] CDR3 usage analysis shows that in the SP both IL-4 treated and untreated mice display similar profiles for the frequency of top ten most read CDR3s (FIG. 6E, upper panel). In the PLN, however, the untreated mice have the highest frequency of the top ten CDR3 reads (FIG. 6E, lower panel). Together, IL-4 treatment seems to influence Vβ and CDR3 usage, both in the SP and the PLN resulting in greater CDR3 diversity in the PLN. This perhaps suggests that IL-4 treatment prevents clonal expansion of specific T cells in this organ. Subsequently, the evolution of the lymphocyte repertoire was analyzed as the mice which reached 12 weeks of age and progressed towards the onset of T1D. Interestingly, the Vβ-Jβ usage profile in the SP was similar in IL-4 recipient and untreated mice (FIG. 7A, upper panel). In fact, the usage of Vβ13 genes was nearly identical between the two groups (FIG. 7B, upper panel). In the PLN, however, although the overall Vβ-Jβ usage was relatively similar in IL-4 treated and untreated mice (FIG. 7A, lower panel), Vβ13 gene usage was lower in IL-4 recipient versus untreated mice (FIG. 7B, lower panel). Further, structural analysis of Vβ genes indicates that nucleotide trimming, while similar in the SP of IL-4 recipient and untreated mice (FIG. 7C, upper panel), there was sizeable reduction in nucleotide trimming in the PLN of IL-4 treated mice (FIG. 7C, lower panel).

[0114] Similarly, N additions, while comparable in both groups in the SP (FIG. 7D, upper panel), there was a notable increase of these events in the T cell of the PLN of IL-4 treated mice

(FIG. 7D, lower panel). Most interestingly, the differential trimming and N additions among the two groups resulted in the usage of longer CDR3s in the PLN T cells of IL-4 treated mice (FIG. 7E). Indeed, while both groups had similar usage of short (27-36 aa) and long (37-45 aa) CDR3s in the SP (FIG. 7E, upper panel), the T cells from IL-4 treated mice were mostly focused in long CDR3s while the T cells of untreated mice used primarily short CDR3s (FIG. 7E, lower panel). Together, IL-4 treatment seems to favor usage of long CDR3s in the PLN, which is consistent with a healthy repertoire in human T1D patients.

Example 6

[0115] Summary of Examples. Type 1 diabetes (T1D) develops spontaneously despite functional antigen presentation machinery in the thymus and a perceptible central tolerance process. Intrathymic enrichment with IL-4 fine-tunes signaling through the IL-4/IL-13 HR in ETPs augments negative selection of self-reactive T cells, sustains a diverse T cell repertoire devoid of clones expressing disease-associated T cell receptor genes, and protects the NOD mouse from T1D. Indeed, optimal IL-4 activates STAT transcription factors to program ETP fate decision towards $CD11c^{+}CD8\alpha^{+}$ dendritic cells agile in negative T cell selection. However, due to diminished iNKT2 cell frequency in NOD thymus, IL-4 is at suboptimal level metering STAT activation to program ETP fate decision towards the T cell lineage leading to diminished negative selection, a clonally restricted TCR repertoire and manifestation of spontaneous T1D. These insights uncover yet another interplay by which IL-4 impacts T1D.

What is claimed is:

1. A method of treatment for an autoimmune disease in a patient, said method comprising a step of increasing a level of interleukin 4 (IL-4) in a thymus of the patient.

2. The method of Claim 1 wherein the autoimmune disease is T cell mediated.

3. The method of Claim 1 wherein the autoimmune disease is Type 1 diabetes.

4. The method of Claim 1 wherein the step of increasing the level of IL-4 comprises injecting IL-4 into the thymus of the patient.

5. The method of Claim 4 wherein between 200 and 500 units of IL-4 are injected into the thymus of the patient once per month for three months.

6. The method of Claim 1 where in the step of increasing the level of IL-4 comprises upregulating the level of IL-4 in the thymus.

7. The method of Claim 6 where upregulating the level of IL-4 in the thymus comprises administering a dose of α-galactosylceramide (αGalCer) to the patient.

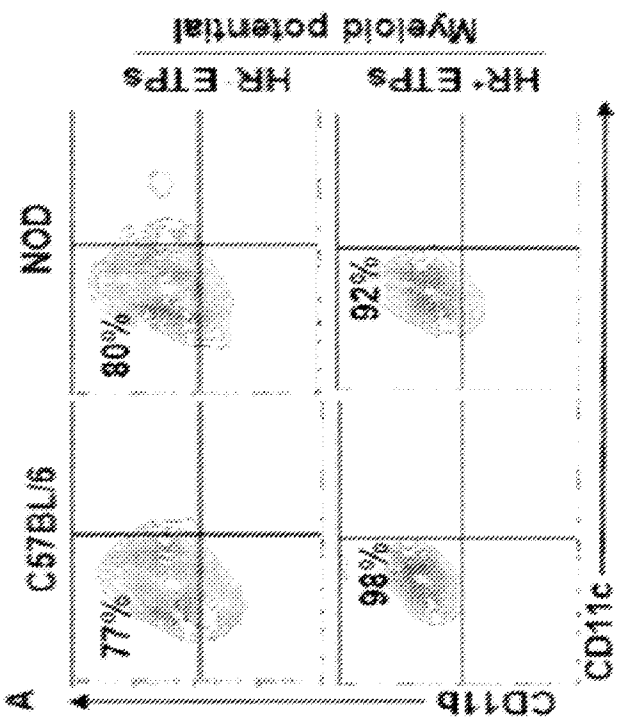

FIG. 1A

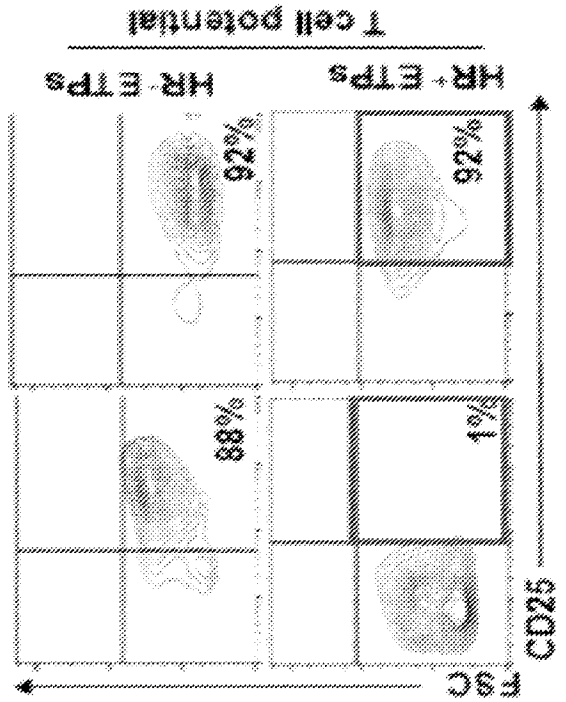

FIG. 1B

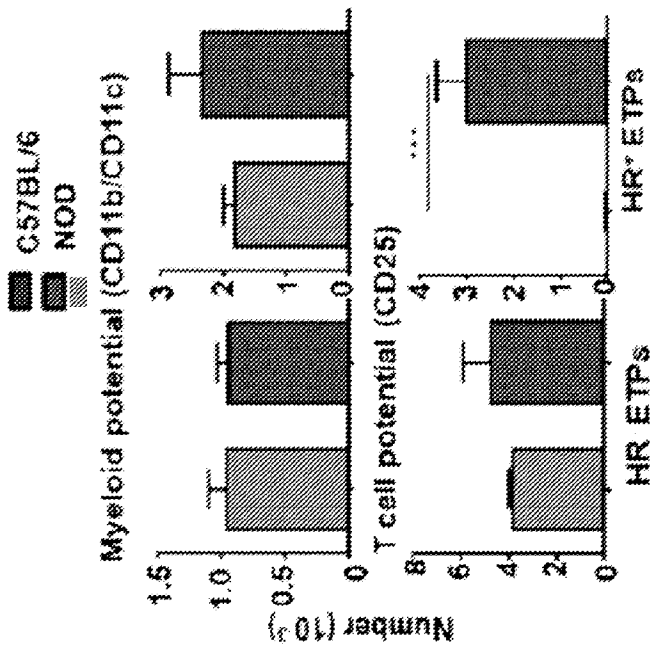

FIG. 1C

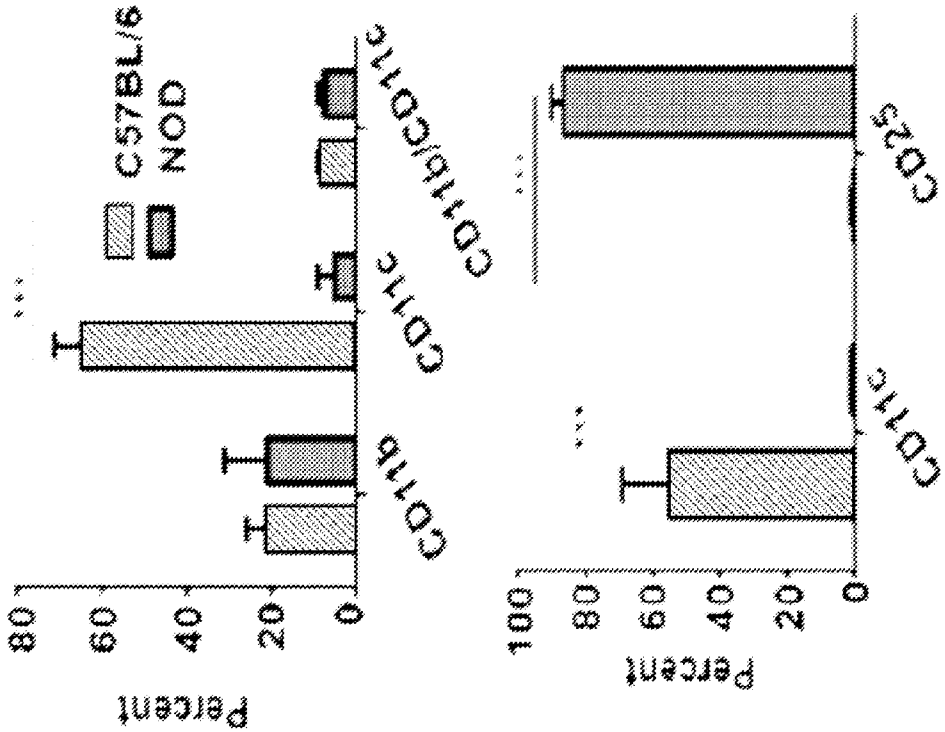
C57BL/6
NOD
CD11b
CD11c
CD11b/CD11c
Percent
0
20
40
60
80
CD25
CD11c
100

FIG. 1E

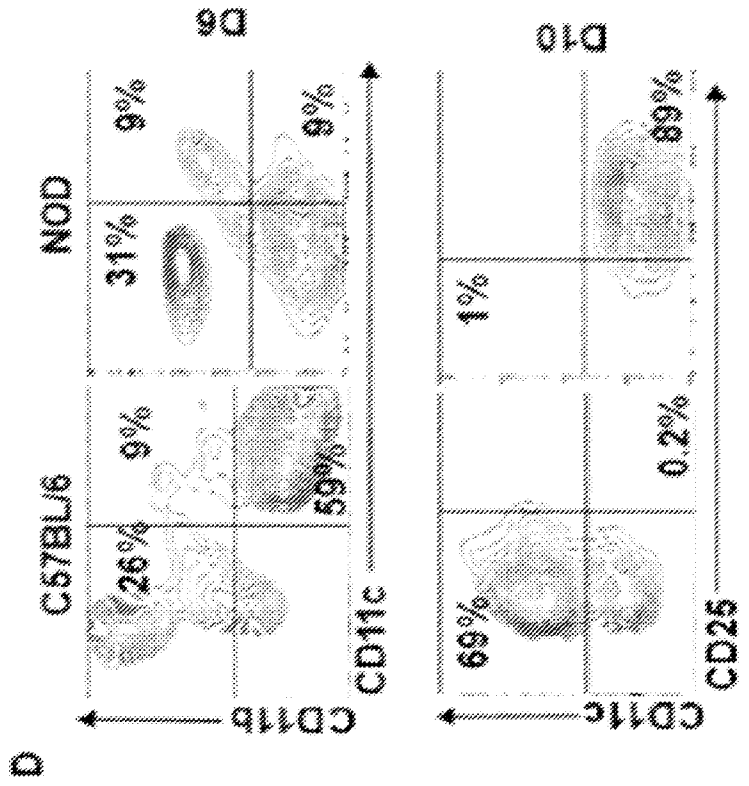
D
C57BL/6
NOD
CD11b
CD11c
26%
9%
59%
31%
9%
9%
D6
D10
CD25
69%
1%
0.2%
89%

FIG. 1D

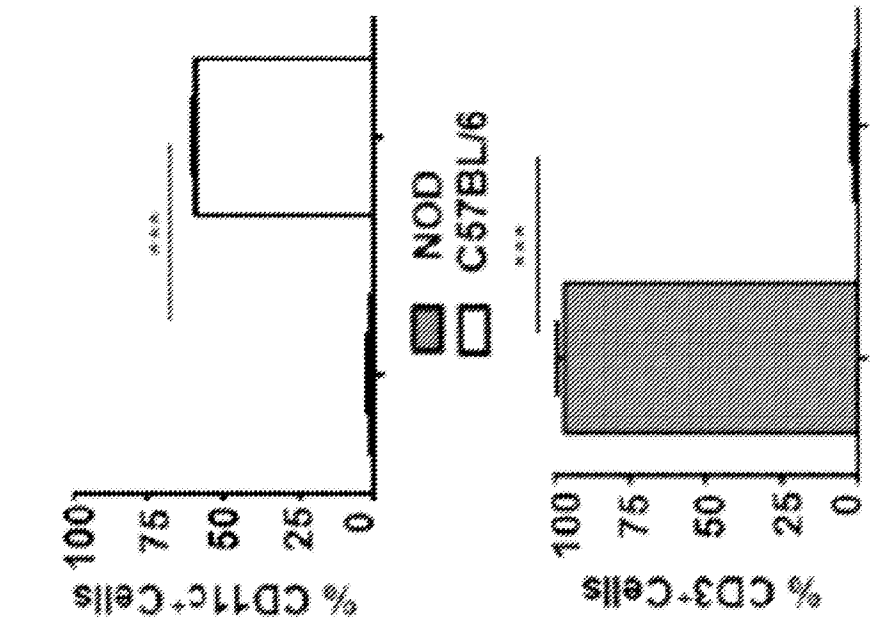
% CD11c+ cells
100
75
50
25
0
***
NOD
C57BL/6
% CD3+ cells
100
75
50
25
0
***

FIG. 2B

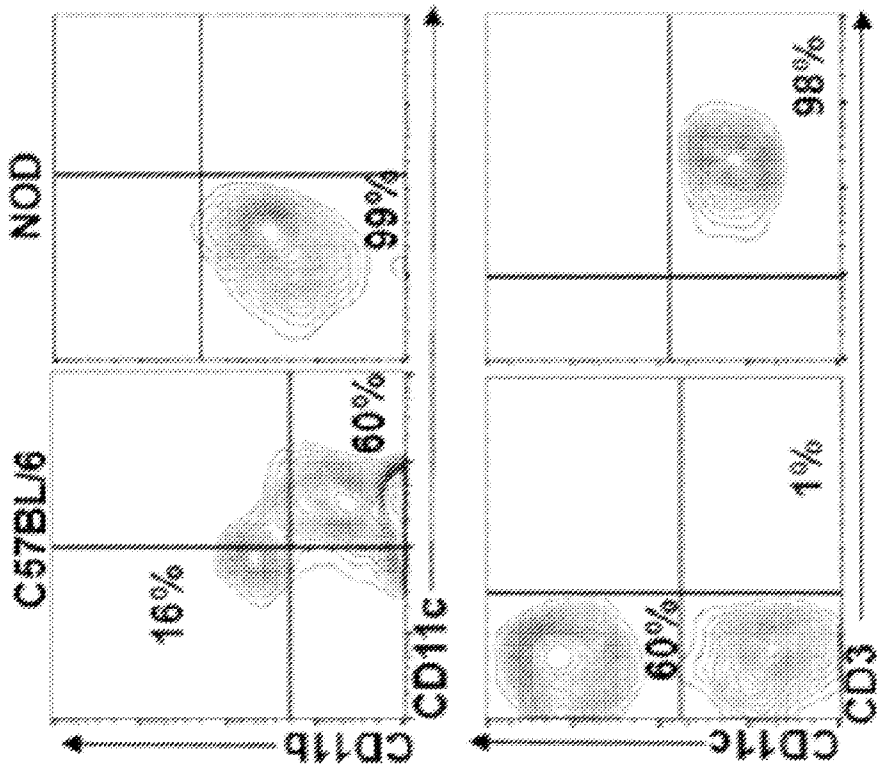
NOD
C57BL/6
99%
60%
16%
CD11b
CD11c
98%
1%
60%
CD11c
CD3

FIG. 2A

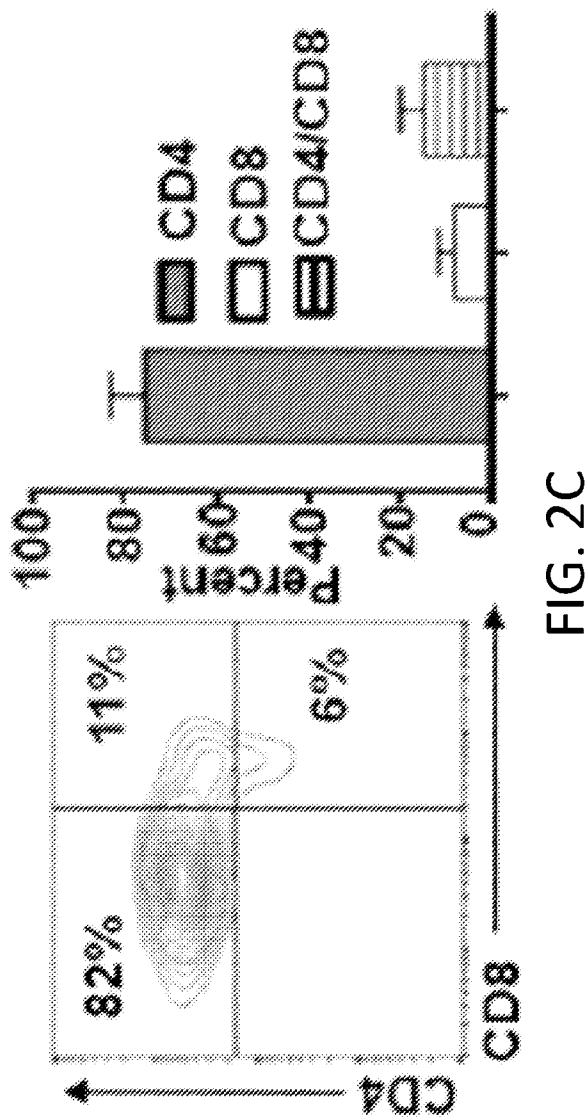
CD4
CD8
CD4/CD8
Percent
100
80
60
40
20
0
11%
6%
82%
CD4
CD8

FIG. 2C

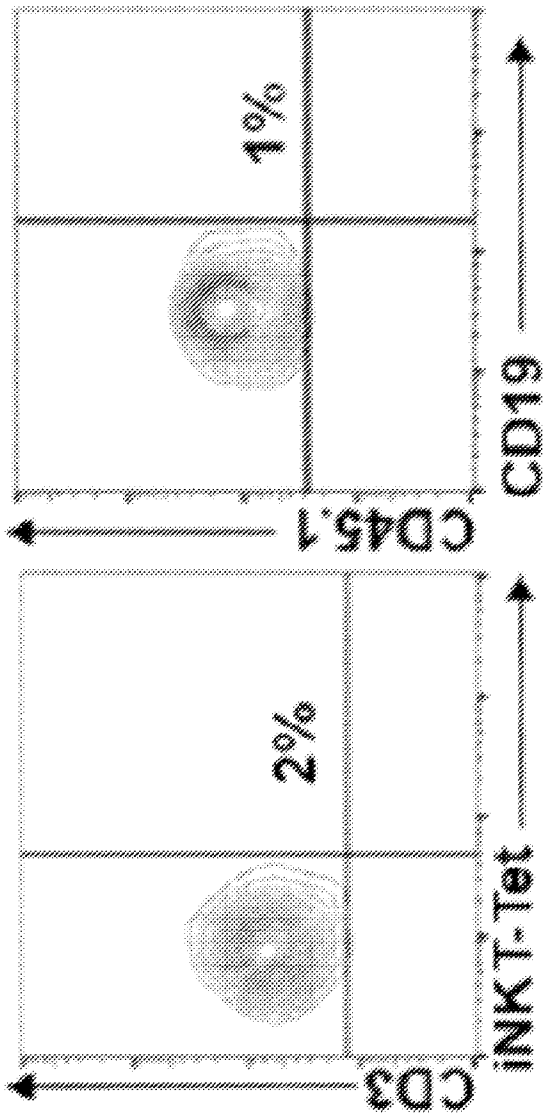
1%
2%
CD45.1
CD19
CD3
iNKT-Tet

FIG. 2D

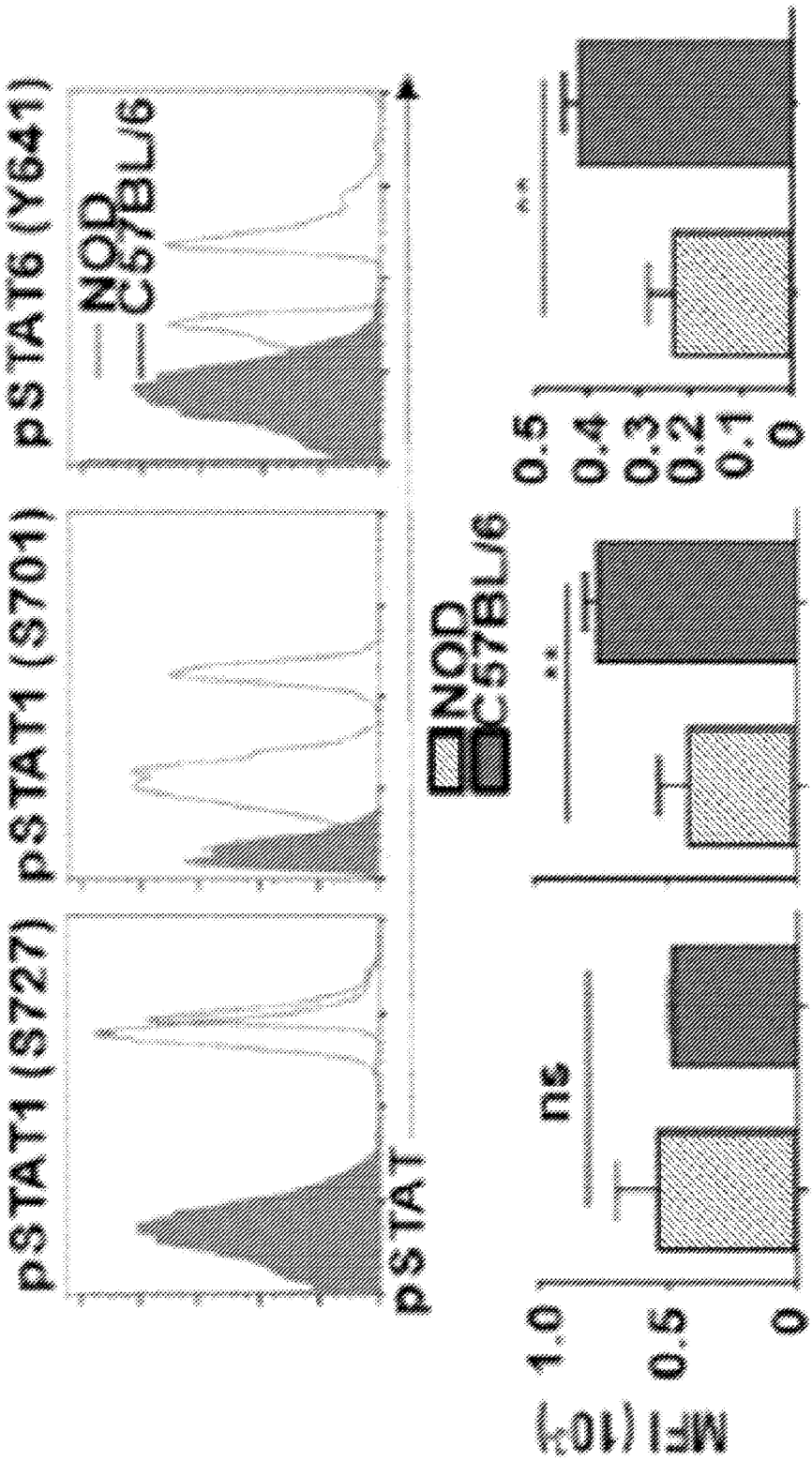
pSTAT1 (S727)
pSTAT1 (S701)
pSTAT6 (Y641)
NOD
C57BL/6
pSTAT
NOD
C57BL/6
MFI (10³)
1.0
0.5
0
ns
**
****
0.5
0.4
0.3
0.2
0.1
0
**
****

FIG. 3A

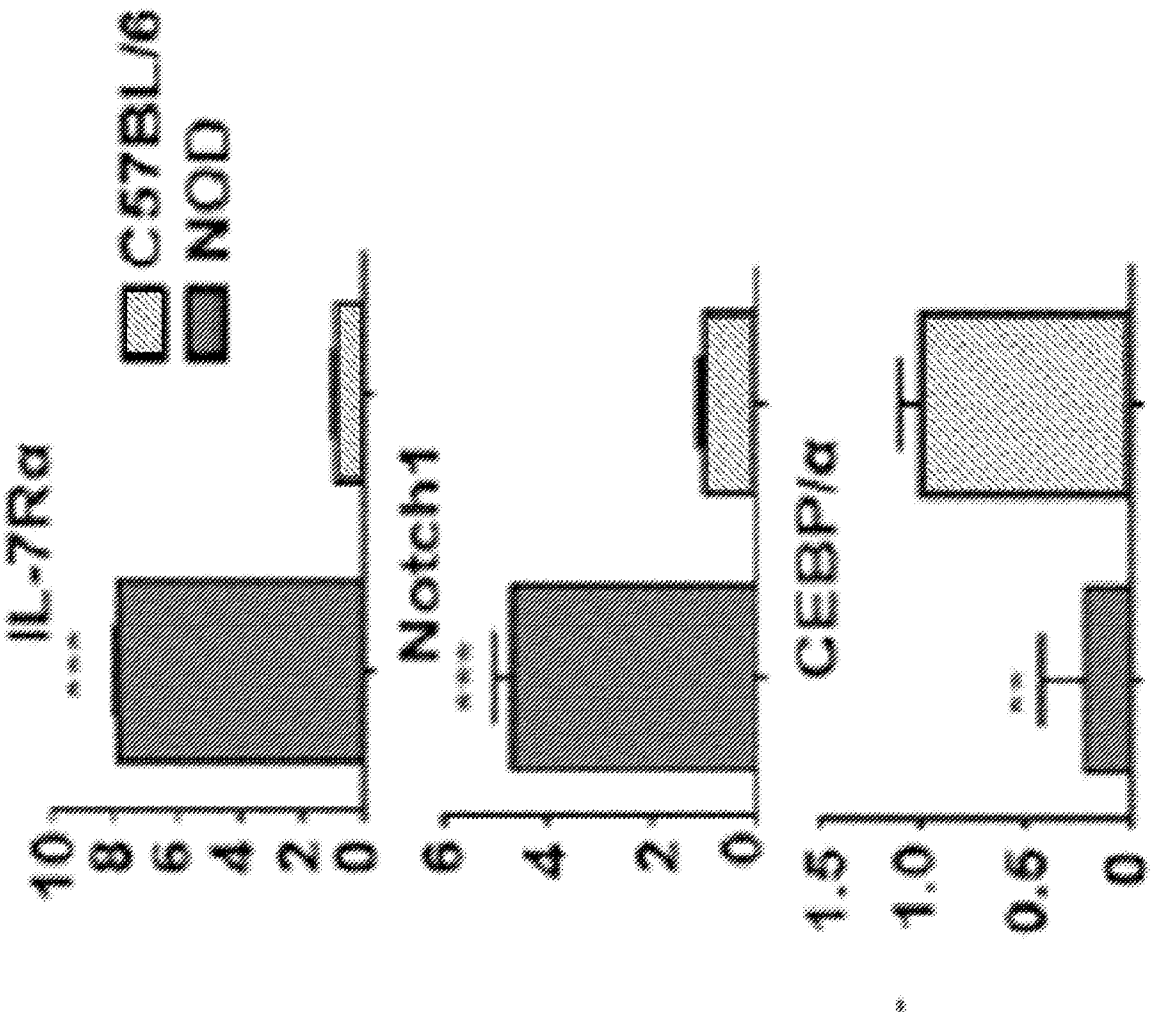

FIG. 3B

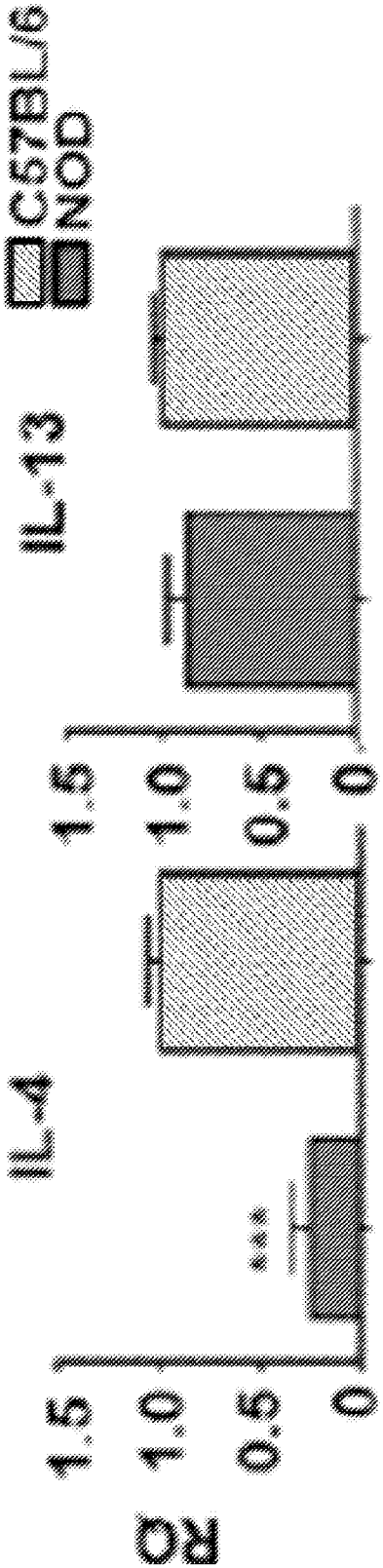
C57BL/6
NOD
IL-13
IL-4
RQ
1.5
1.0
0.5
0
***

FIG. 3C

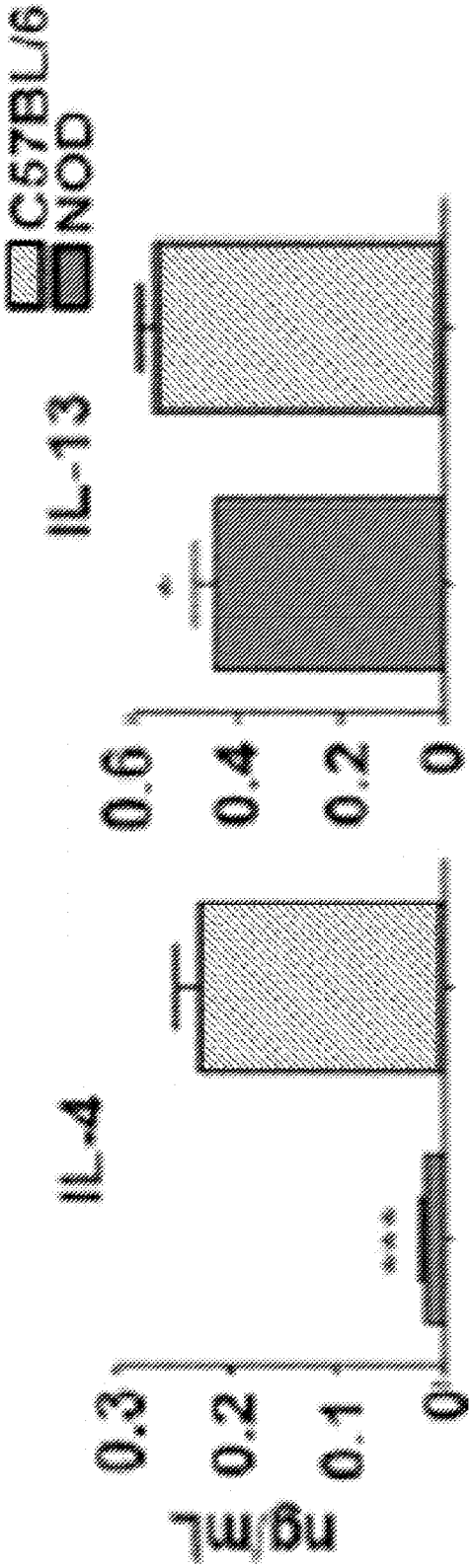
C57BL/6
NOD
IL-13
IL-4
ng/mL
0.6
0.4
0.2
0
0.3
0.2
0.1
0
*
***

FIG. 3D

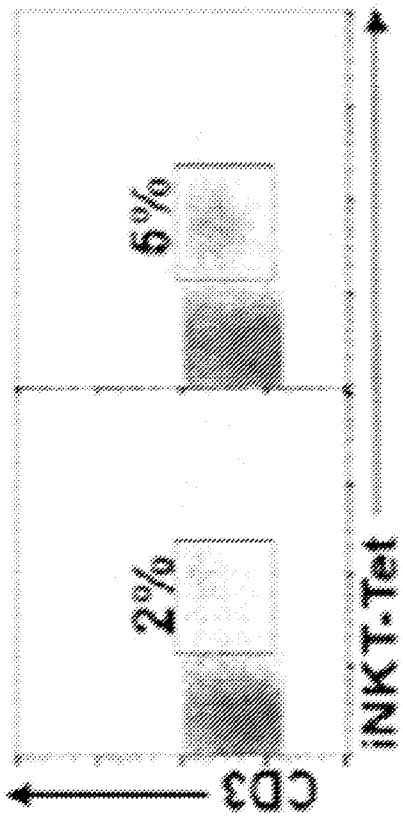

FIG. 3E

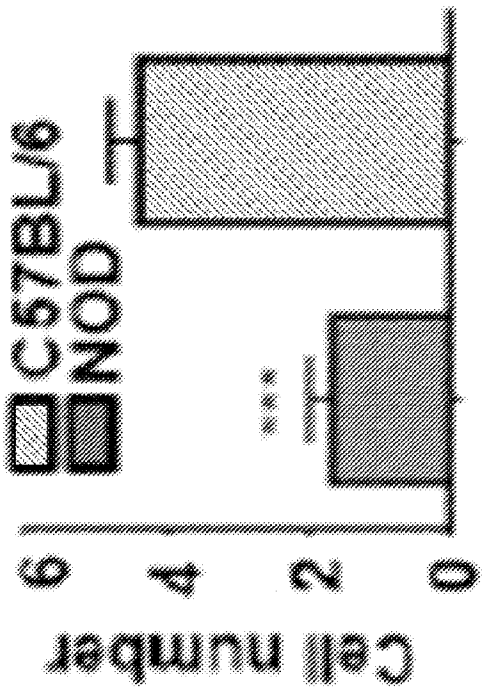

FIG. 3F

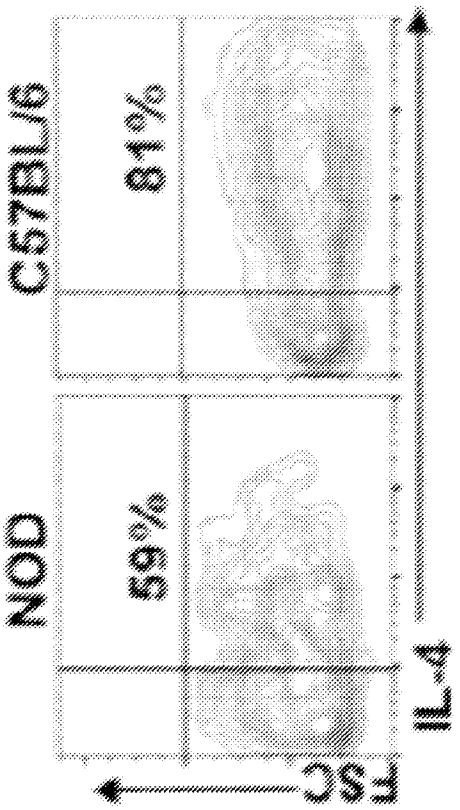
C57BL/6
81%
NOD
59%
IL-4
FSC

FIG. 3G

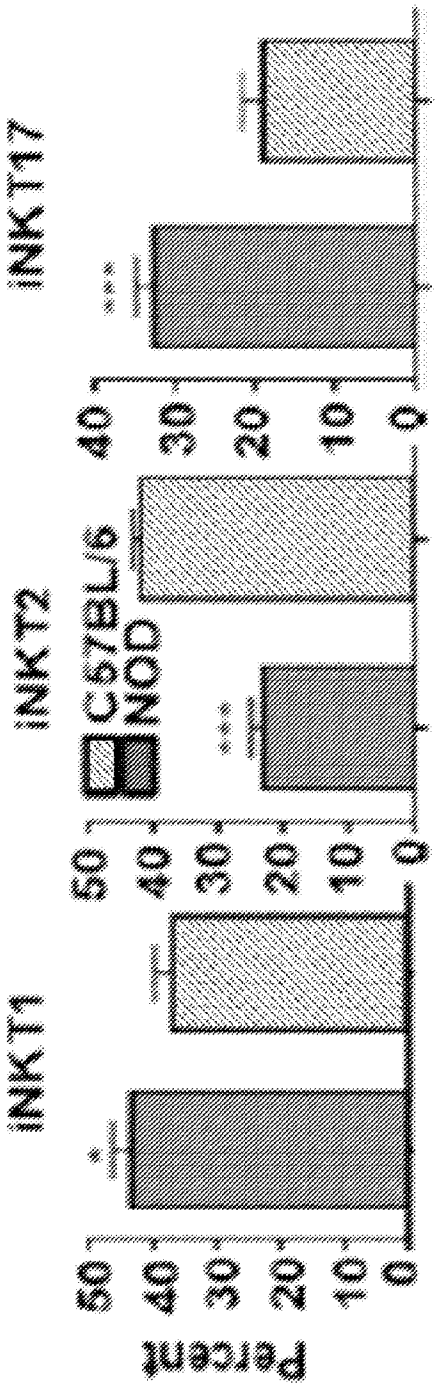
iNKT17
iNKT2
C57BL/6
NOD
iNKT1
Percent
60
40
30
20
10
0

FIG. 3H

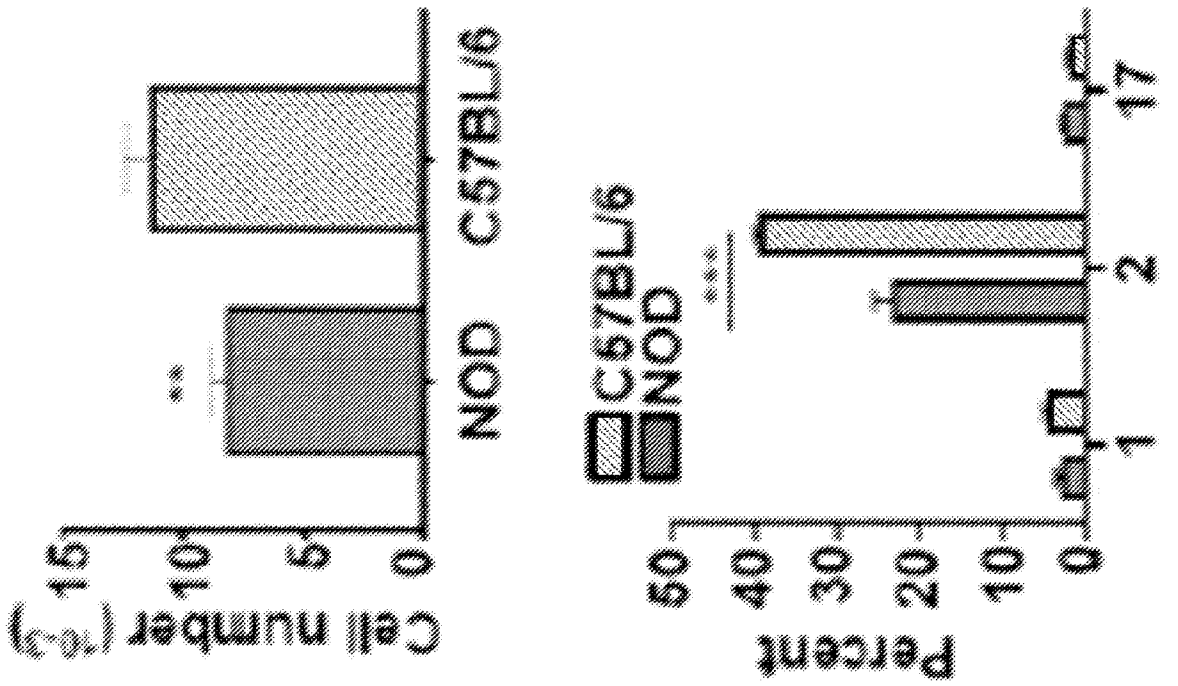
Cell number (10^3)
15
10
5
0
NOD
C57BL/6
Percent
60
40
30
20
10
0
C57BL/6
NOD
1
2
17

FIG. 3I

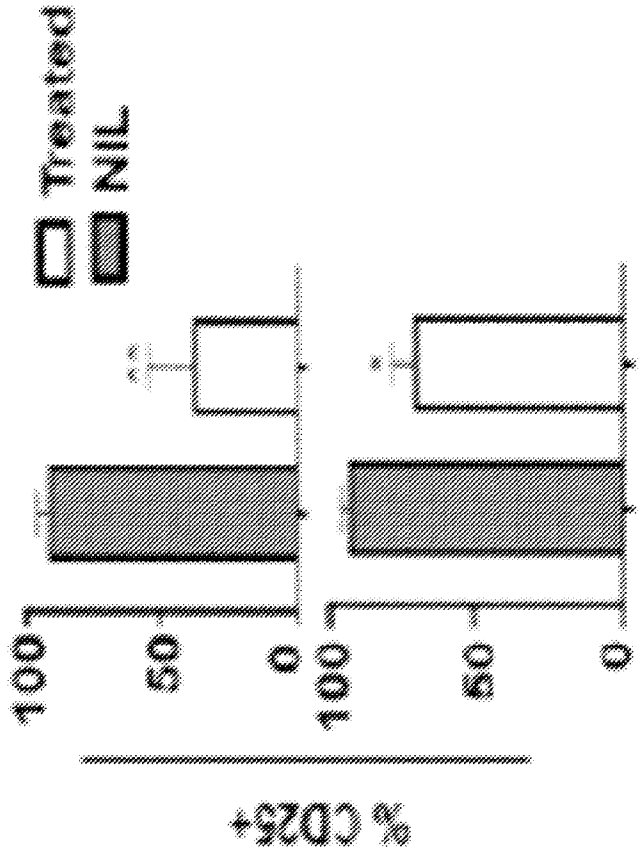
Treated
NIL
100
60
0
100
60
0
% CD25+

FIG. 4B

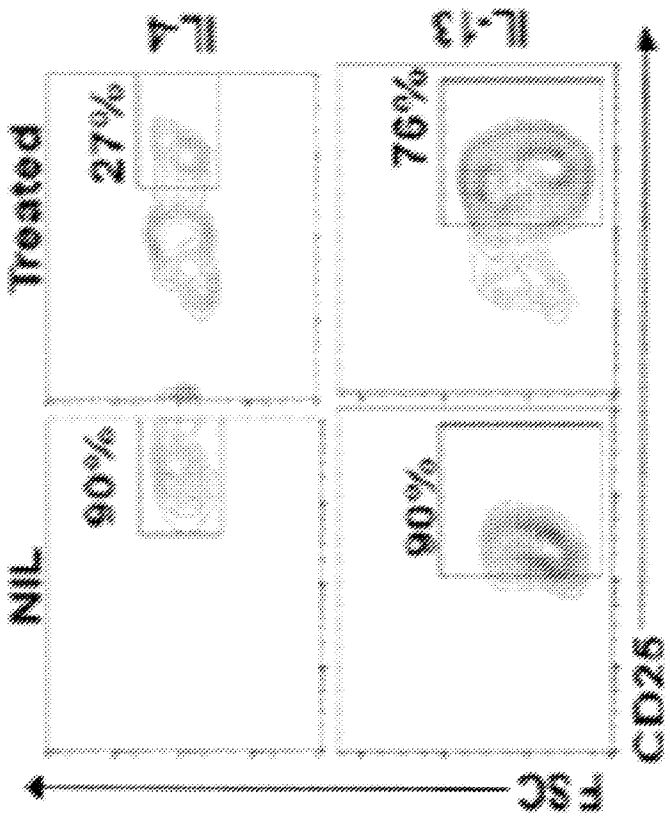
IL-4
IL-13
Treated
27%
76%
NIL
90%
90%
CD25
FSC

FIG. 4A

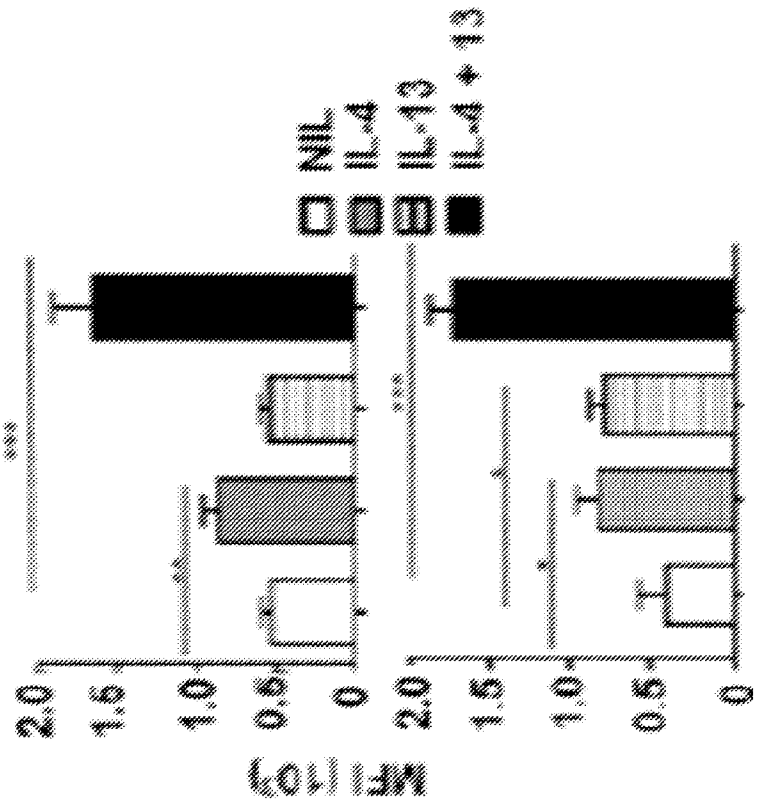
Nil
IL4
IL13
IL4 + 13
***
***
2.0
1.5
1.0
0.5
0
MFI (103)

FIG. 4D

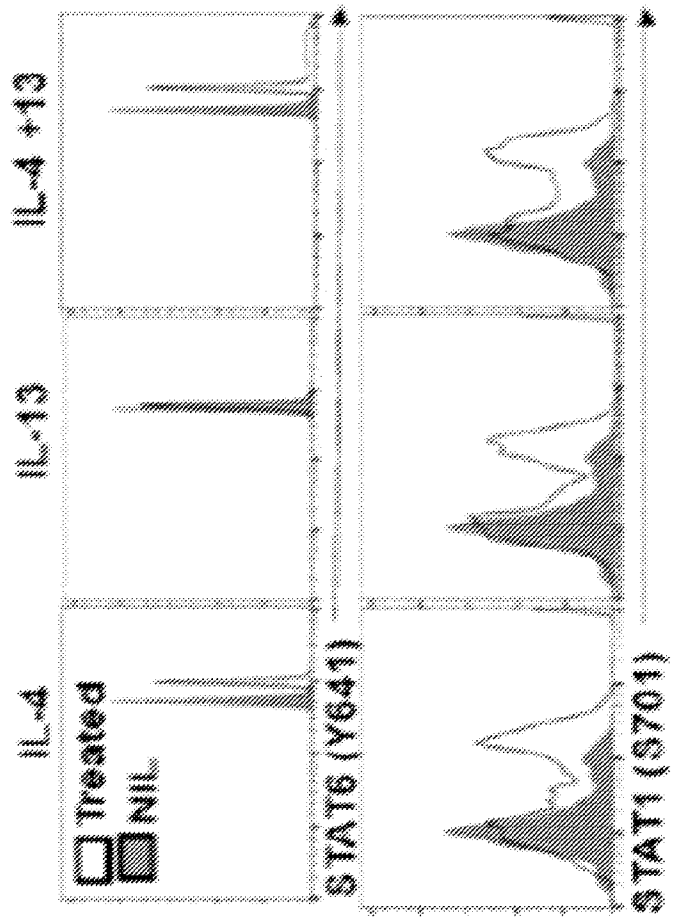
IL_4
IL_13
IL_4 +13
Treated
Nil
STAT6 (Y641)
STAT1 (S701)

FIG. 4C

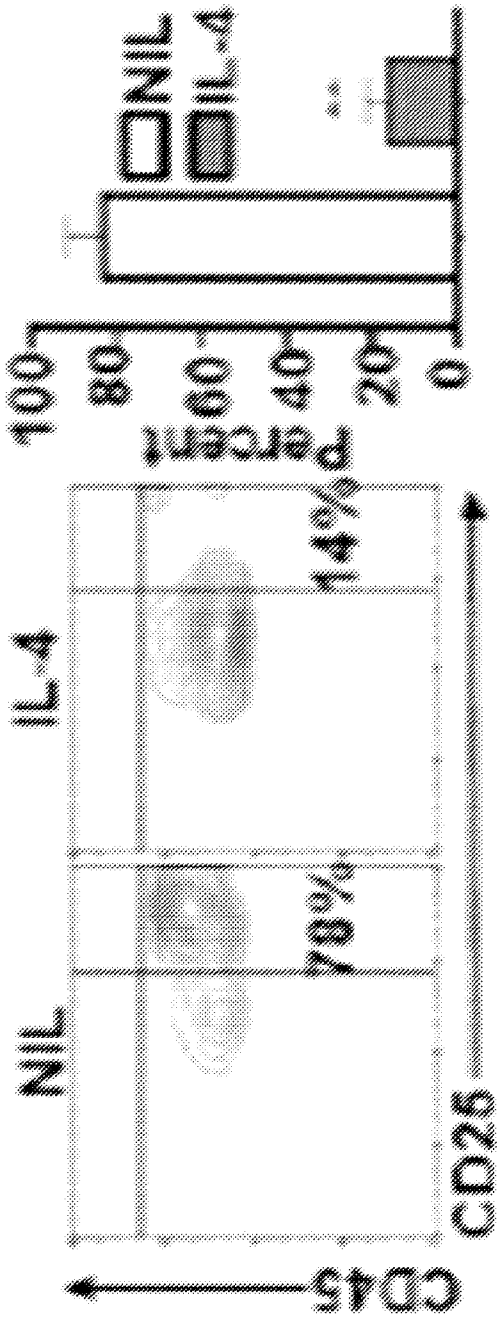
NIL
IL-4
100
80
60
40
20
0
Percent
IL-4
NIL
14%
78%
CD26
CD45

FIG. 4E

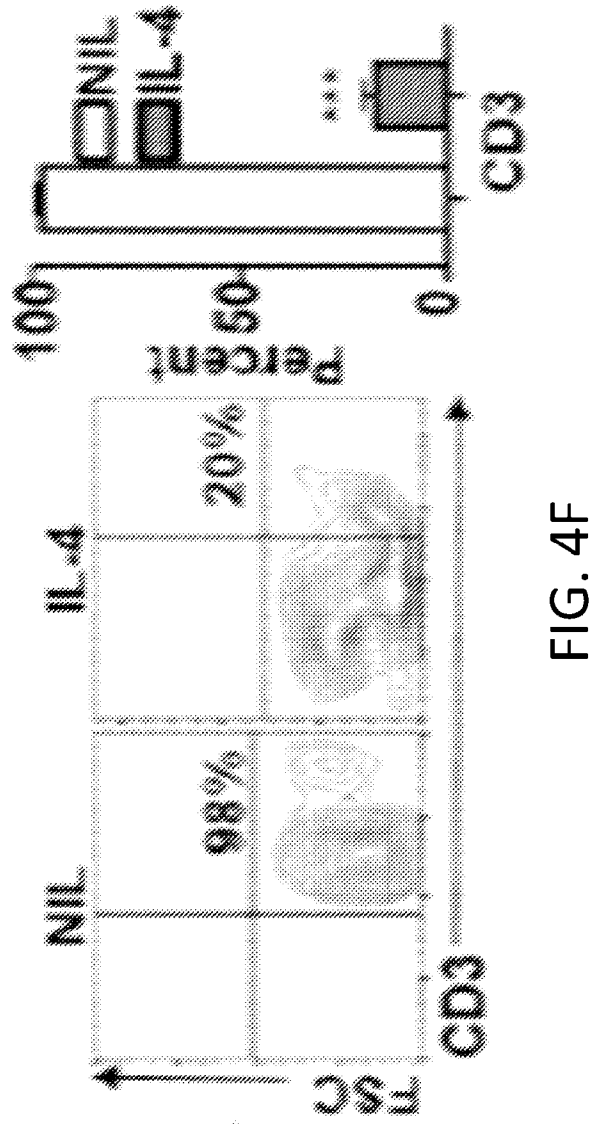
NIL
IL-4
100
60
0
Percent
CD3
IL-4
NIL
20%
98%
CD3
FSC

FIG. 4F

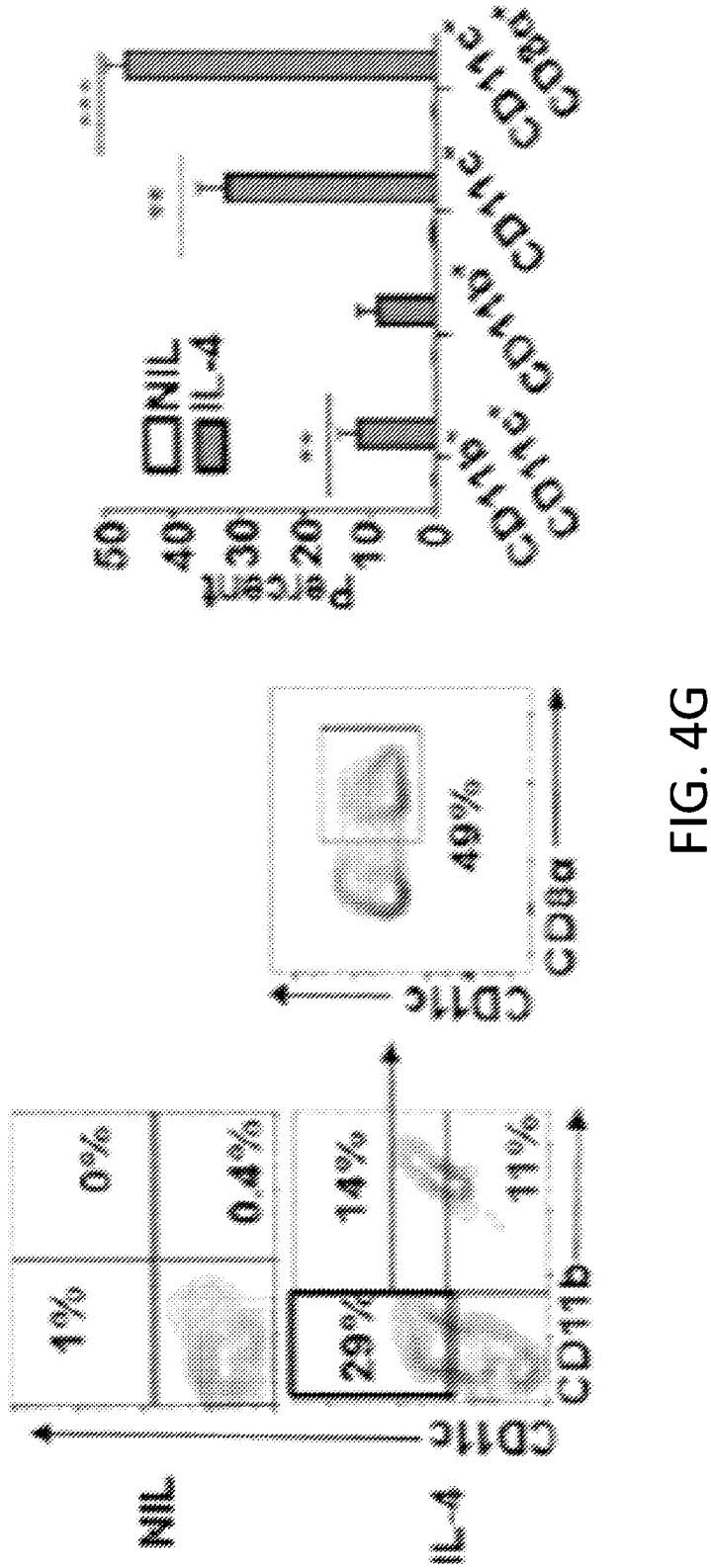
NIL
IL-4
CD11c
CD11b
1%
0%
29%
0.4%
14%
11%
CD11c
CD8α
49%
Percent
60
40
30
20
10
0
CD11c+ CD11b+
CD11c+ CD11b-
CD11c- CD11b+
CD11c- CD11b-
**
**
***

FIG. 4G

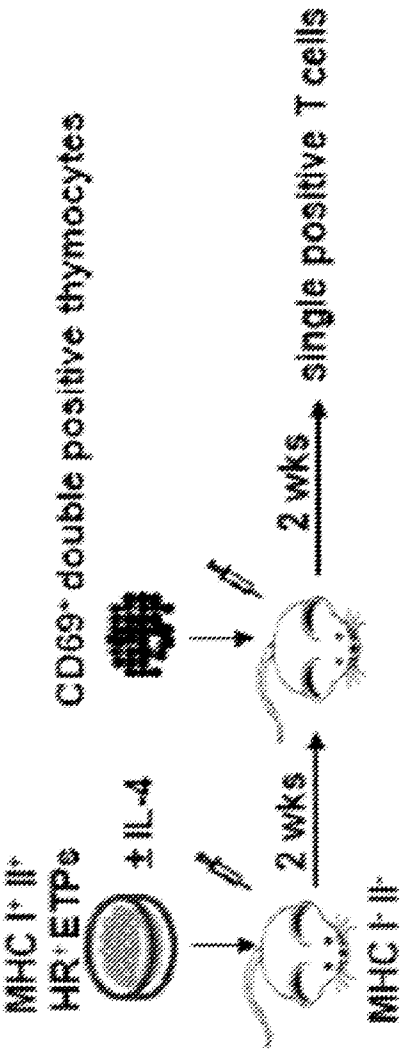

FIG. 5A

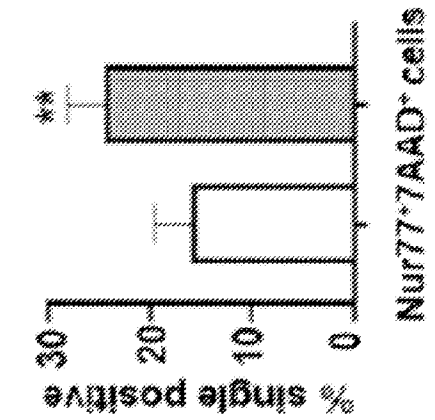

FIG. 5C

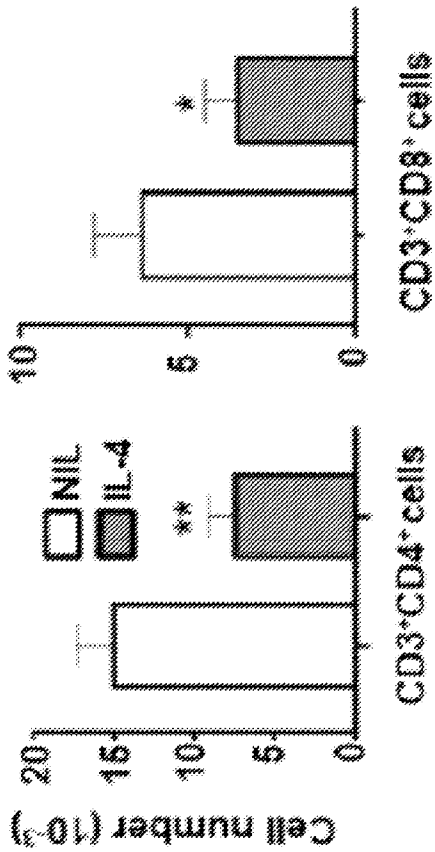

FIG. 5B

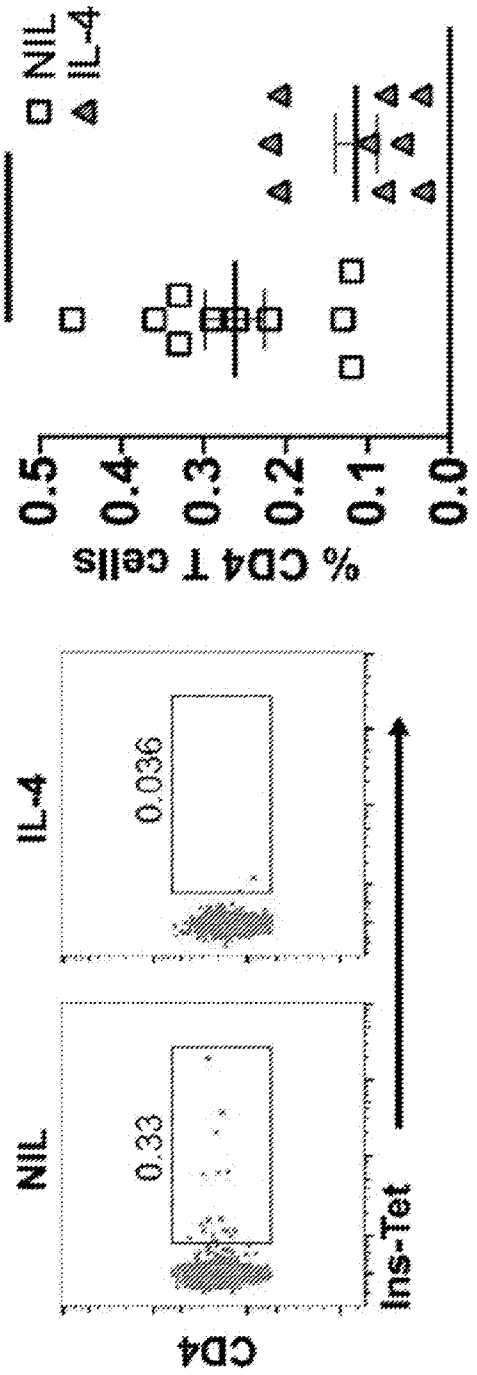
NIL
IL-4
0.036
0.33
Ins-Tet
CD4
**
% CD4 T cells
0.5
0.4
0.3
0.2
0.1
0.0

FIG. 5D

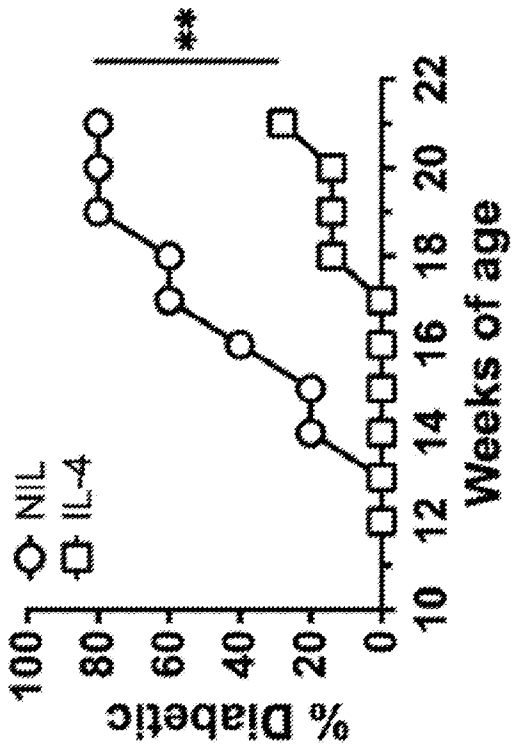
**
NIL
IL-4
% Diabetic
100
80
60
40
20
0
10
12
14
16
18
20
22
Weeks of age

FIG. 5E

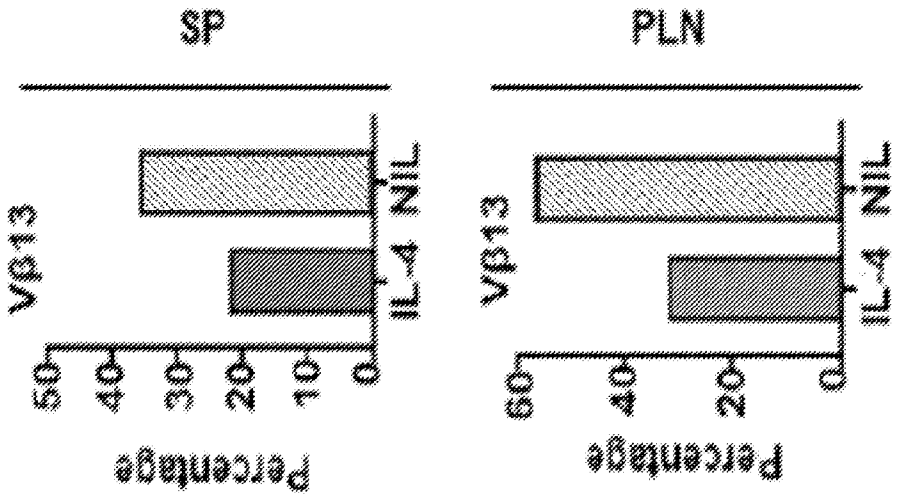
SP
PLN
Vβ13
IL-4
NIL
Percentage
60
40
30
20
10
0

FIG. 6B

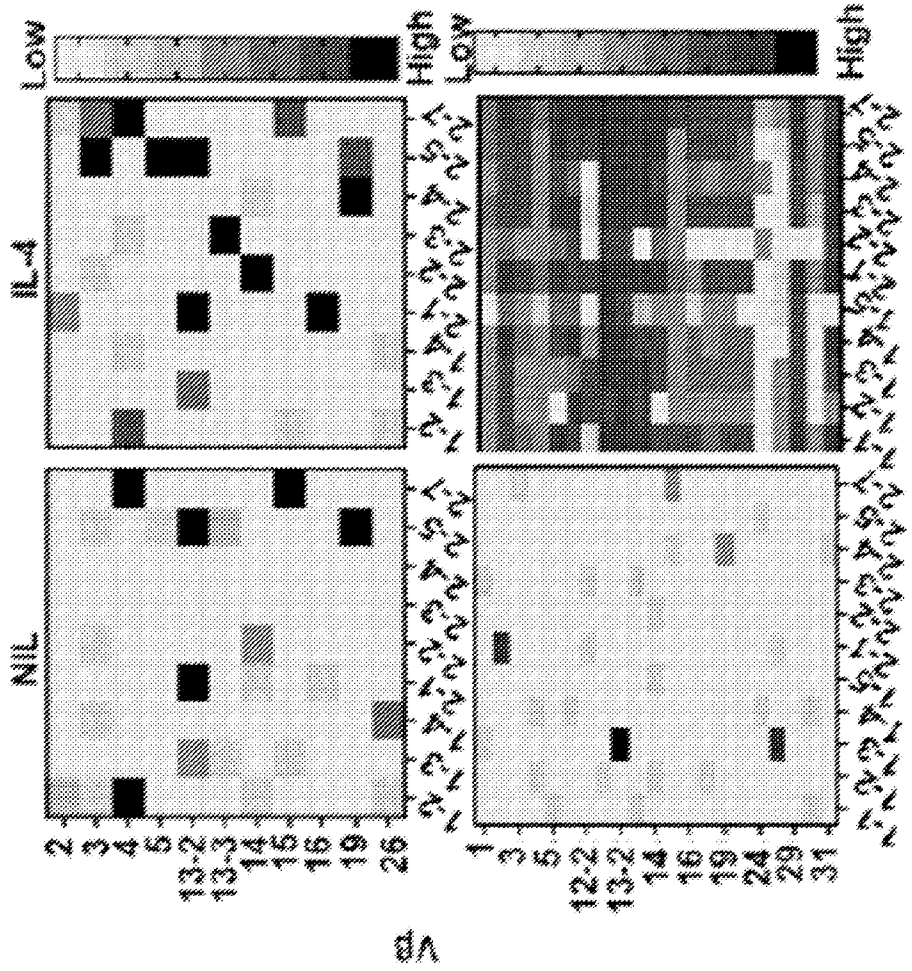
Low
High
IL-4
NIL
Vβ

FIG. 6A

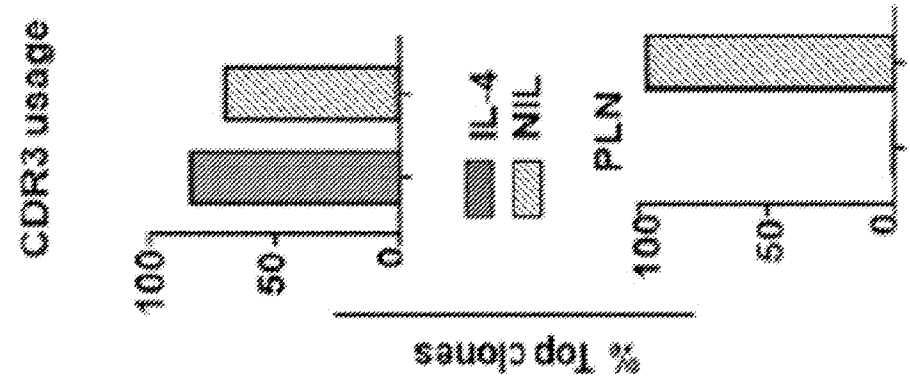

FIG. 6E

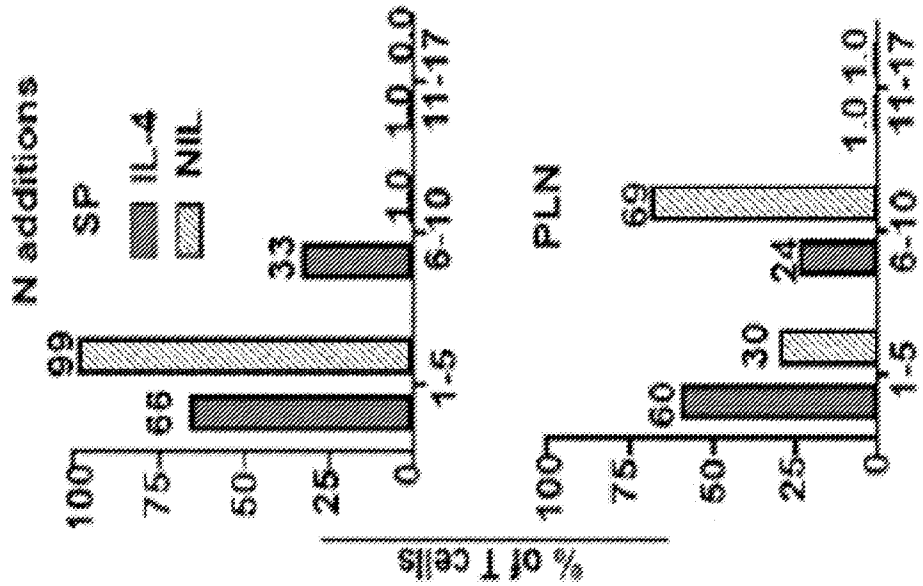

FIG. 6D

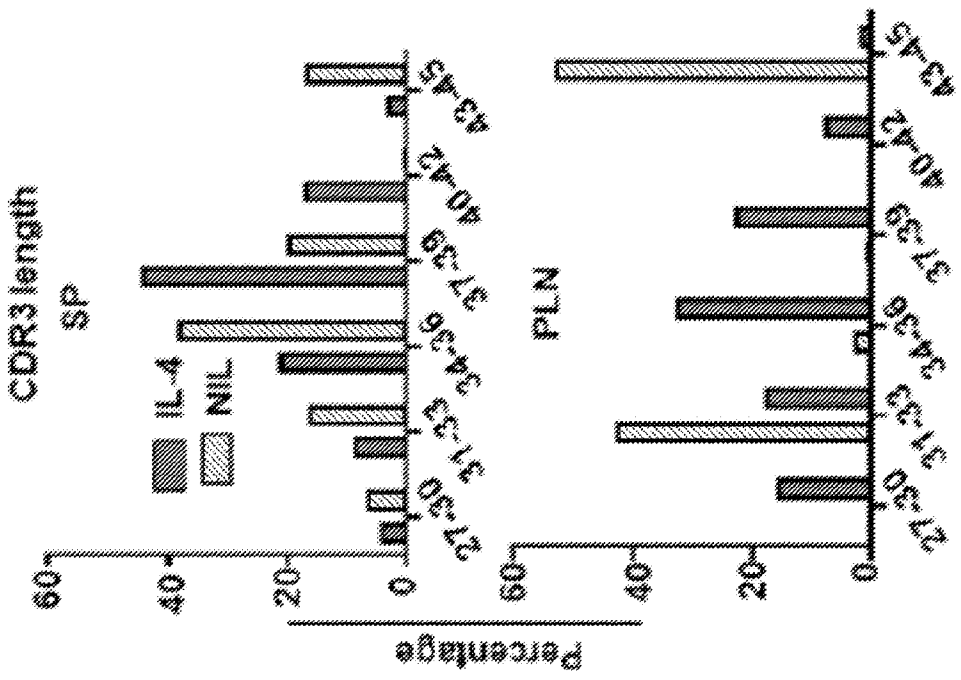

FIG. 6C

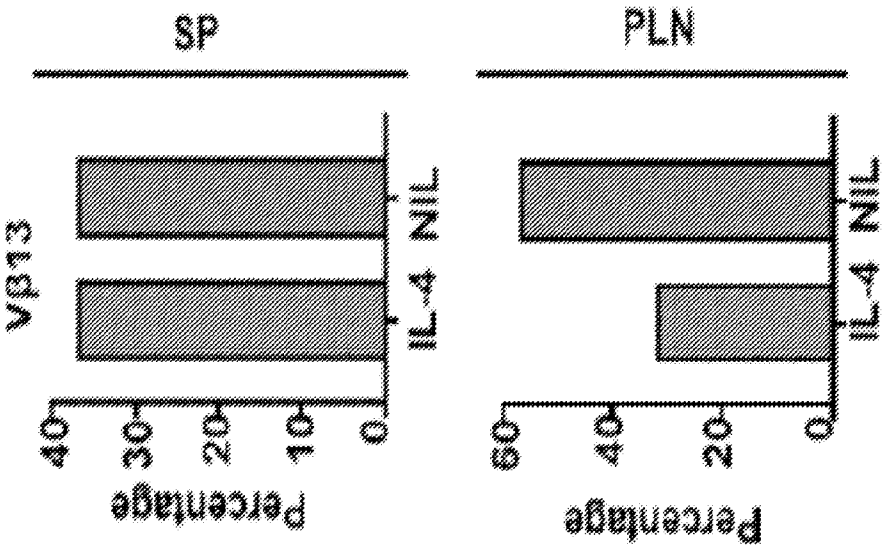
SP
PLN
Vβ13
IL-4
NIL
Percentage
40
30
20
10
0
60
40
20
0

FIG. 7B

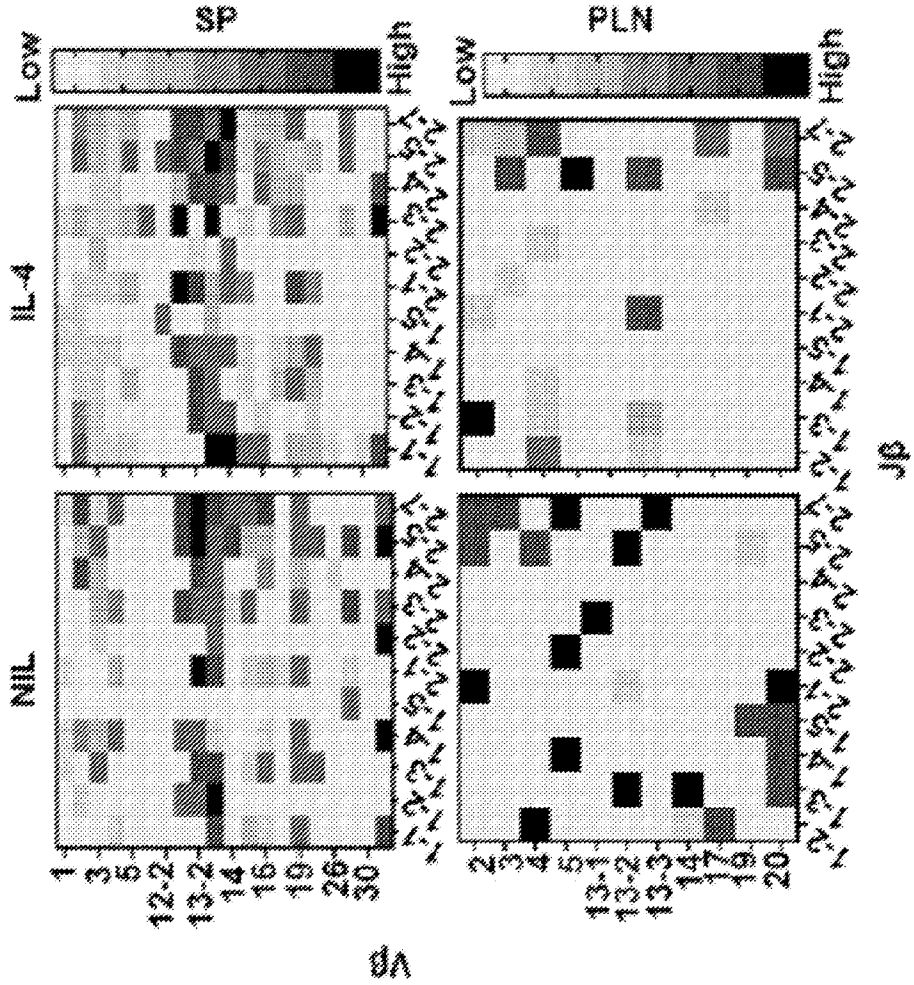
SP
PLN
Low
High
IL-4
NIL
Vβ
Jβ

FIG. 7A

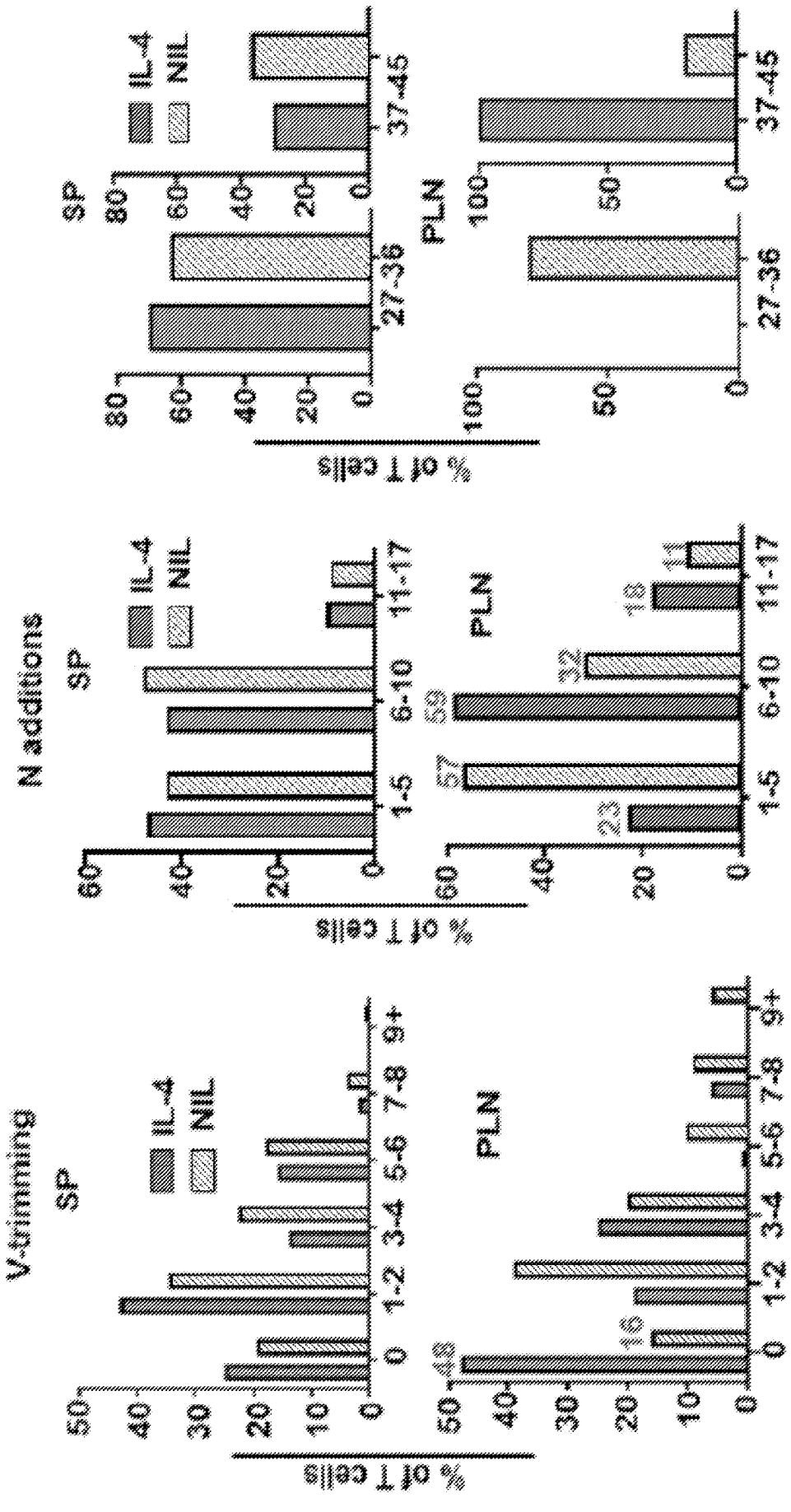

FIG. 7C

FIG. 7D

FIG. 7E

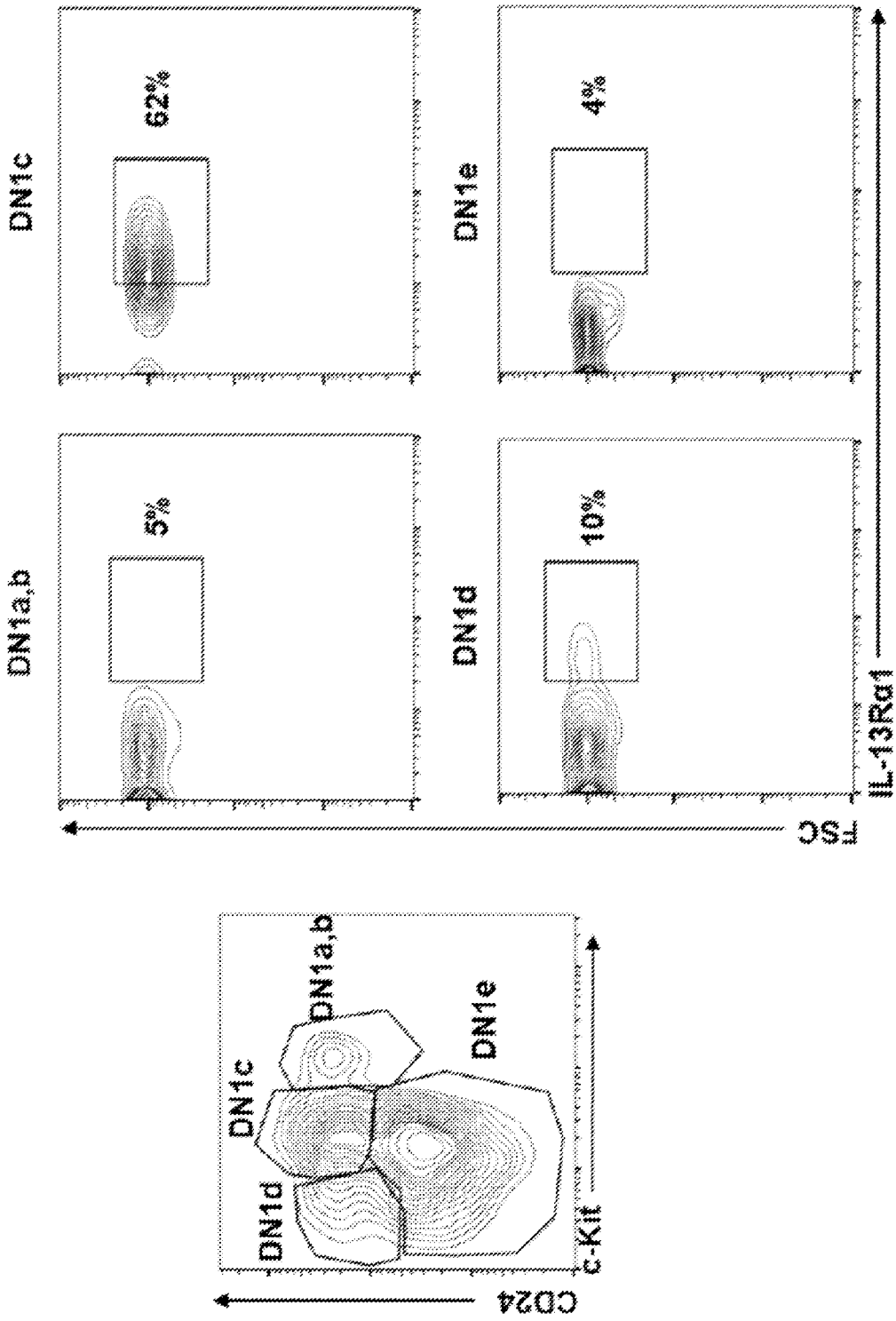
DN1c
62%
DN1e
4%
DN1a,b
5%
DN1d
10%
FSC
IL-13Rα1
DN1a,b
DN1e
DN1c
DN1d
c-Kit
CD24

FIG. 8A

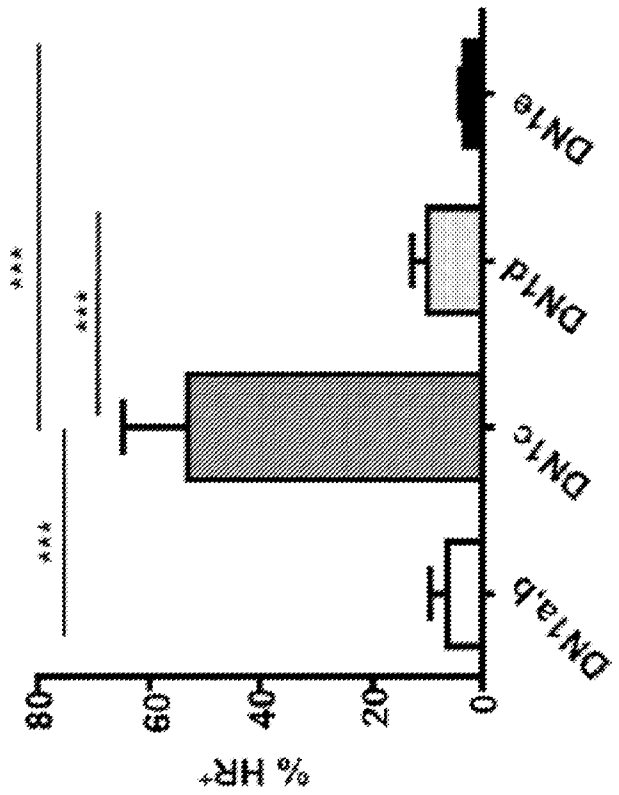

FIG. 8B

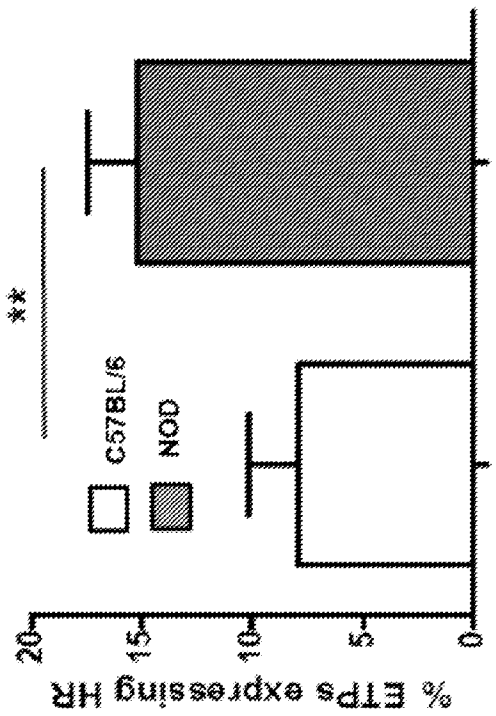

FIG. 9A

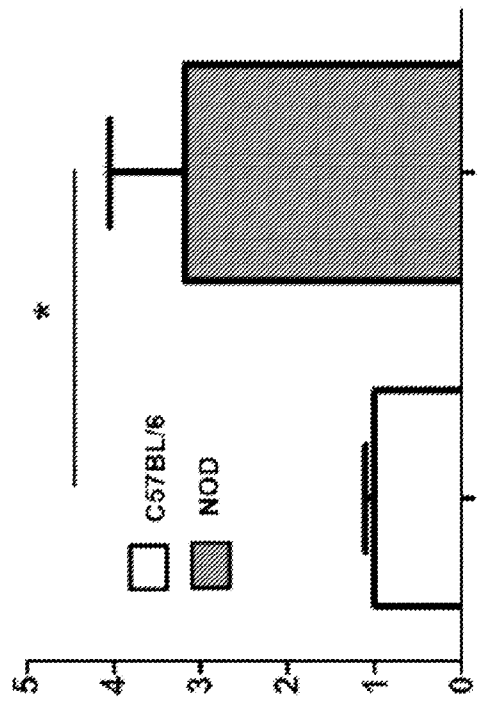

FIG. 9B

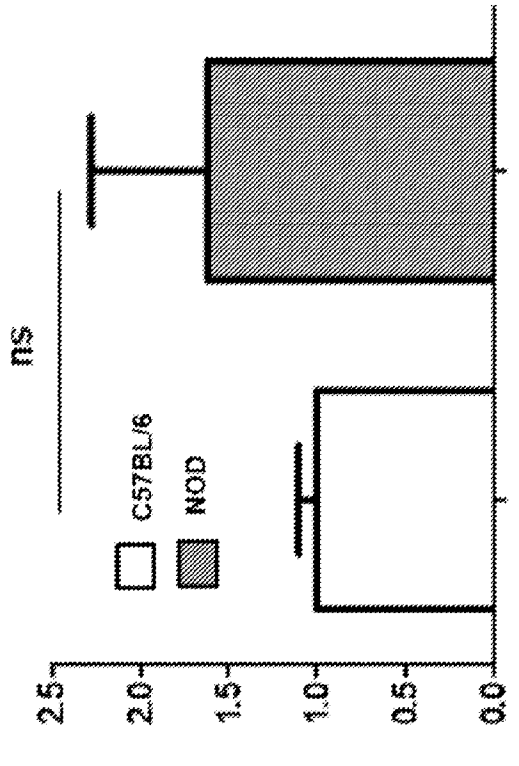

FIG. 9C

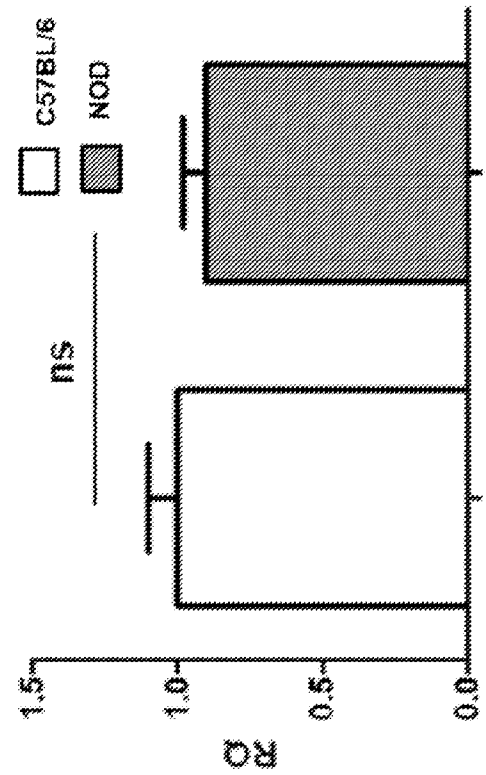

FIG. 9D

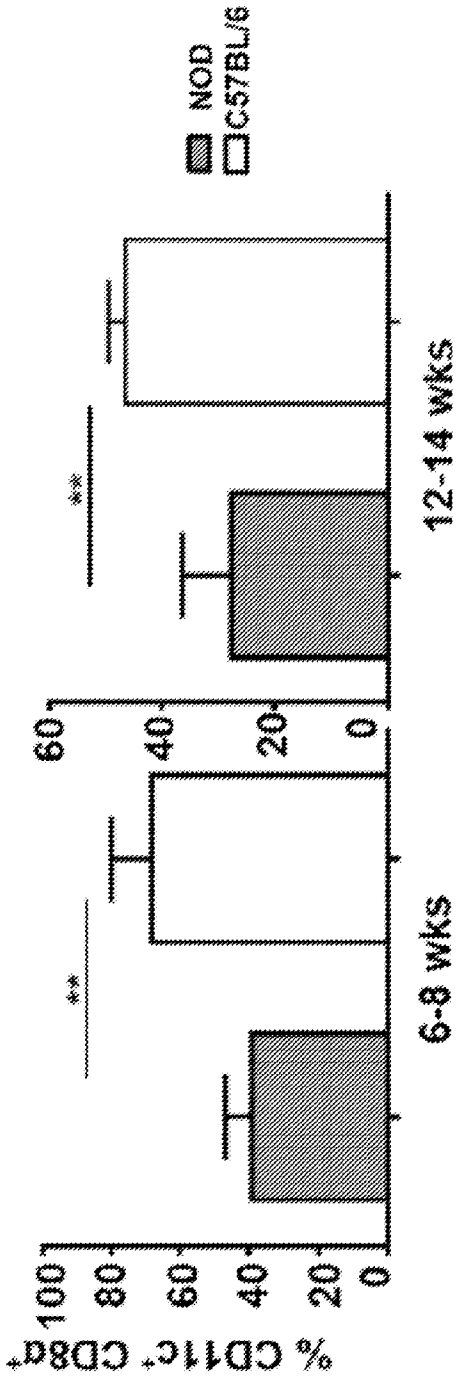

FIG. 10A

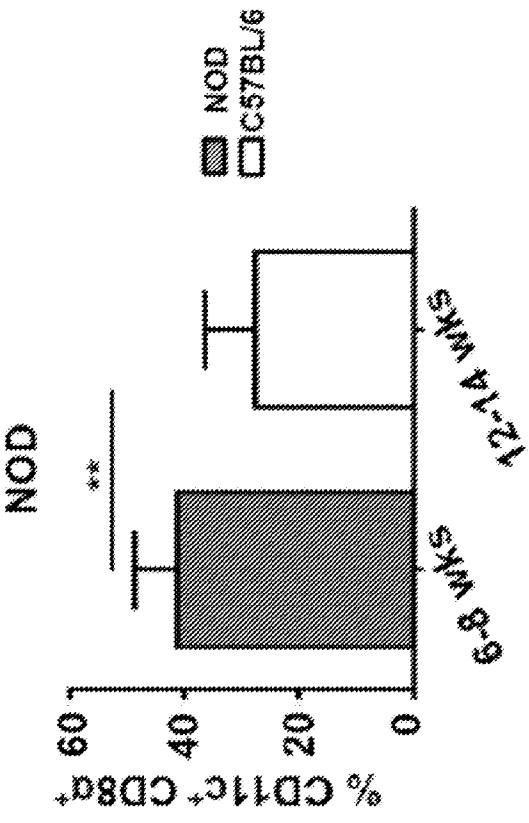

FIG. 10B

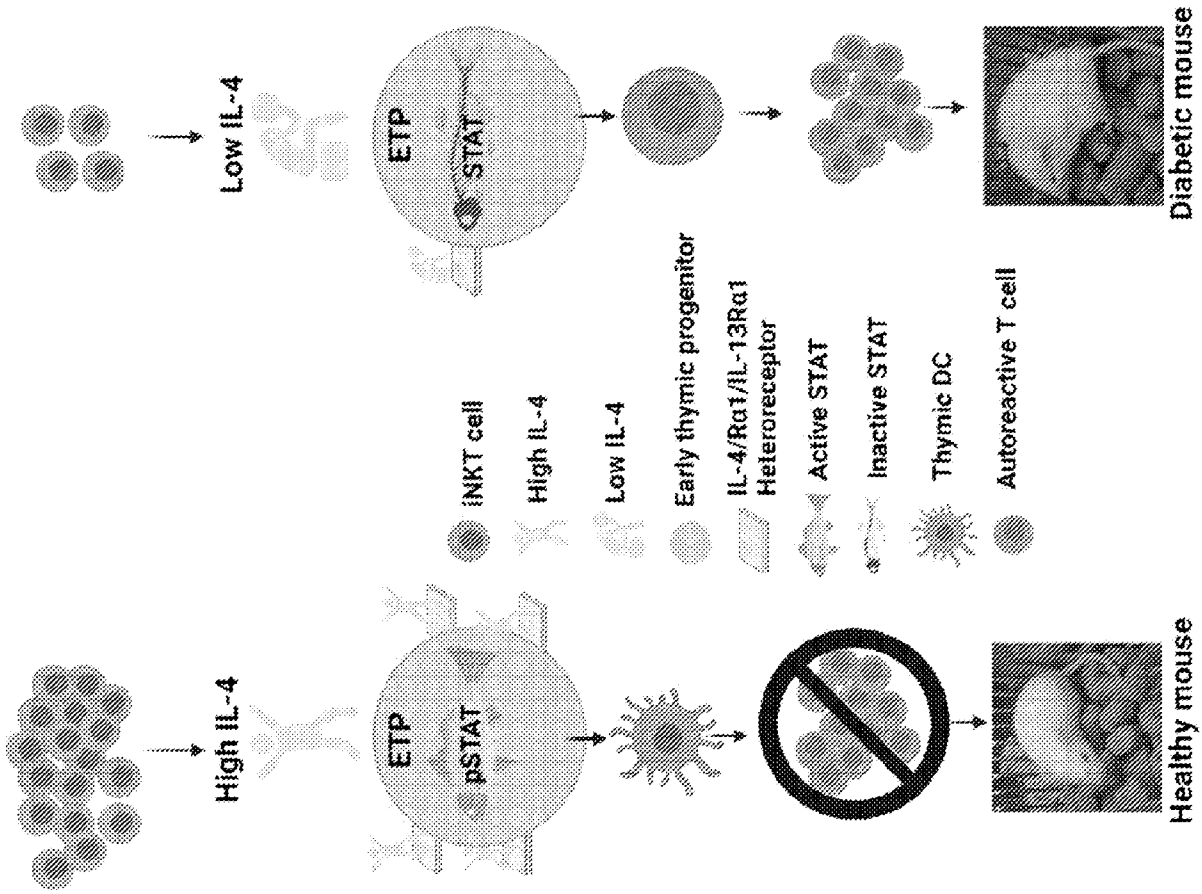
High IL-4
ETP
pSTAT
Healthy mouse
Low IL-4
ETP
STAT
Diabetic mouse
iNKT cell
High IL-4
Low IL-4
Early thymic progenitor
IL-4/Rα1/IL-13Rα1 Heteroreceptor
Active STAT
Inactive STAT
Thymic DC
Autoreactive T cell

FIG. 11

INTERNATIONAL SEARCH REPORT

International application No.
PCT/US2024/041786

A. CLASSIFICATION OF SUBJECT MATTER

IPC: ***A61K 38/20*** (2024.01); ***A61P 3/10*** (2024.01); ***C07K 14/54*** (2024.01); *A61P 37/00* (2024.01)

CPC: ***A61K 38/2026; A61P 3/10; C07K 14/5406;*** *A61P 37/00*

According to International Patent Classification (IPC) or to both national classification and IPC

B. FIELDS SEARCHED

Minimum documentation searched (classification system followed by classification symbols)

See Search History Document

Documentation searched other than minimum documentation to the extent that such documents are included in the fields searched

See Search History Document

Electronic data base consulted during the international search (name of data base and, where practicable, search terms used)

See Search History Document

C. DOCUMENTS CONSIDERED TO BE RELEVANT

Category*	Citation of document, with indication, where appropriate, of the relevant passages	Relevant to claim No.
Y	US 2010/0104590 A1 (KANG et al.) 29 April 2010 (29.04.2010) entire document	7
A	US 2020/0345676 A1 (EPITRACKER INC.) 05 November 2020 (05.11.2020) entire document	1-7
A	US 2003/0220229 A1 (GRIFFIN et al.) 27 November 2003 (27.11.2003) entire document	1-7
X	CAMERON et al. "IL-4 prevents insulitis and insulin-dependent diabetes mellitus in nonobese diabetic mice by potentiation of regulatory T helper-2 cell function," J Immunol, 15 November 1997 (15.11.1997), Vol. 159(10), Pgs. 4686-4692. entire document	1-3, 6
Y		7
A	RAPOPORT et al. "Interleukin 4 reverses T cell proliferative unresponsiveness and prevents the onset of diabetes in nonobese diabetic mice," J Exp Med, July 1993 (07.1993), Vol. 178, Pgs. 87-99. entire document	1-7

☐ Further documents are listed in the continuation of Box C. ☐ See patent family annex.

* Special categories of cited documents:
"A" document defining the general state of the art which is not considered to be of particular relevance
"D" document cited by the applicant in the international application
"E" earlier application or patent but published on or after the international filing date
"L" document which may throw doubts on priority claim(s) or which is cited to establish the publication date of another citation or other special reason (as specified)
"O" document referring to an oral disclosure, use, exhibition or other means
"P" document published prior to the international filing date but later than the priority date claimed
"T" later document published after the international filing date or priority date and not in conflict with the application but cited to understand the principle or theory underlying the invention
"X" document of particular relevance; the claimed invention cannot be considered novel or cannot be considered to involve an inventive step when the document is taken alone
"Y" document of particular relevance; the claimed invention cannot be considered to involve an inventive step when the document is combined with one or more other such documents, such combination being obvious to a person skilled in the art
"&" document member of the same patent family

Date of the actual completion of the international search	Date of mailing of the international search report
22 September 2024 (22.09.2024)	**10 October 2024 (10.10.2024)**

Name and mailing address of the ISA/US	Authorized officer
Mail Stop PCT, Attn: ISA/US **Commissioner for Patents** **P.O. Box 1450, Alexandria, VA 22313-1450**	**MATOS** **TAINA**
Facsimile No. **571-273-8300**	Telephone No. **571-272-4300**

INTERNATIONAL SEARCH REPORT

International application No.
PCT/US2024/041786

Box No. I Nucleotide and/or amino acid sequence(s) (Continuation of item 1.c of the first sheet)

1. With regard to any nucleotide and/or amino acid sequence disclosed in the international application, the international search was carried out on the basis of a sequence listing:
   a. ☑ forming part of the international application as filed.
   b. ☐ furnished subsequent to the international filing date for the purposes of international search (Rule 13*ter*.1(a)),
      ☐ accompanied by a statement to the effect that the sequence listing does not go beyond the disclosure in the international application as filed.

2. ☐ With regard to any nucleotide and/or amino acid sequence disclosed in the international application, this report has been established to the extent that a meaningful search could be carried out without a WIPO Standard ST.26 compliant sequence listing.

3. Additional comments: